TAMPEREEN
AMMATTIKORKEAKOULU

SYNTHESIS, CHARACTERIZATION AND APPLICATION OF HYDROPHOBIC ZEOLITES

Rulis Heidari

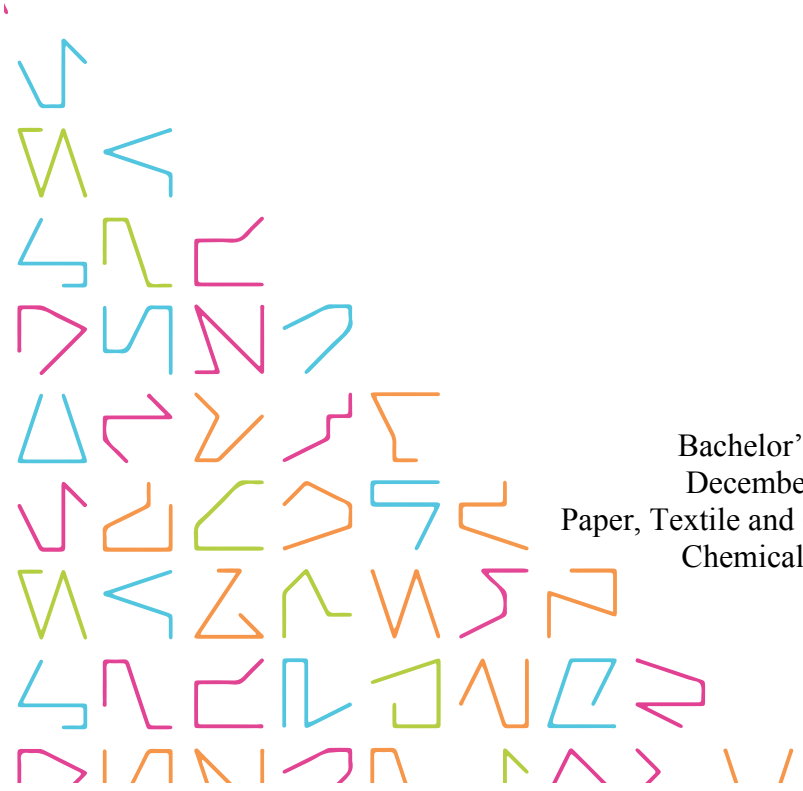

Bachelor's thesis
December 2016
Paper, Textile and Chemical Engineering
Chemical Engineering

TIIVISTELMÄ

Tampereen ammattikorkeakoulu
Paperi-, tekstiili- ja kemiantekniikan koulutusohjelma
Kemiantekniikka

HEIDARI RULIS:
Hydrofobisten zeoliittien synteesi, luonnehdinta ja sovelluksia

Opinnäytetyö 54 sivua, joista liitteitä 7 sivua
Joulukuu 2016

Tämän opinnäytetyön tarkoituksena oli suunnitella ja syntetisoida zeoliitti, joka on hydrofobinen ja omaa oikeanlaisen huokoskoon. Tuotetta on tarkoitus käyttää etanolin absorboimiseen vesiliuoksesta.

Työn kirjallisessa osassa käsitellään zeoliitin historiaa, ominaisuksia, rakenteita, sen sovelluksia, bioetanolin fermentointia ja adsorptioisotermejä. Kokeellinen osa tehtiin kahdella eri järjestelmällä: hydroksidiperusjärjestelmällä ja vetyfluoridineutraalijärjestelmällä. Piioksidin zeoliitin oletetaan olevan hyvin hydrofobinen ja korkeasti huokoinen. Työssä suunniteltiin ja syntetisoitiin neljä erilaista huokoskokoja omaavia piioksidin zeoliitteja. Lisäksi testattiin niiden adsorptio etanolin laimeassa vesiliuoksessa. Zeoliitin luonnehdinta suoritettiin käyttämällä röntgensädediffraktio-mittauslaitetta ja analysointielektronimikroskooppia käytettiin kuvien morfologiseen käsittelyyn ja typen adsorption-desorptiota adsorption analyysiin. Etanolin adsorptio laimeasta liuoksesta tehtiin käyttämällä etanoli-vesiliuosta. Zeoliittinäytteet analysoitiin liekki-ionisaatiodetektorilla (FID) varustetulla kaasukromatografialla niiden etanolipitoisuuden testaamiseksi.

Röntgensädediffraktion avulla osoitettiin näytteiden yhteys pentasil-ryhmään kuuluvan zeoliitin kehystyyppi-MFI:n kiteisyyteen ja niiden puhtauteen. Analysointielektronimikroskoopilla (SEM) kuvattiin morfologian kidekokoa välillä 1.0–5.0 μm ja 100–200 nm. Typen adsorption-desorption isotermillä osoitettiin materiaalin tyyppiä (tyypi-1 isotermi eli Langmuirin adsorptioisotermi) ja huokoskokoa. Adsorption testauksella osoitettiin, että hydrofobiset zeoliitit olivat parempia kuin yleisimmät zeoliitit. Hydrofobisia zeoliiteja voidaan käyttää muun muassa orgaanisten aineiden poistossa vedestä, alkoholin adsorptiossa vedestä ja yleisen pyykinpesuaineissa vedenpehmentimenä. Pyykinpesuaineissa adsorptio on fysikaalinen adsorptio, joka tapahtuu van der Waalsin voimalla, heikoilla vuorovaikutuksilla, ja jonka kyky perustuu adsorption pintaan. Zeoliiteilla on suuri pinta-ala, josta on hyötyä molekyylin pinta-adsorptiolle. Hydrofobiset zeoliitit ovat potentiaalinen sovellusmahdollisuus bioetanolin fermentointiin.

Asiasanat: Adsorptio, etanoli, zeoliitti, ioninvaihto, ZSM-5

ABSTRACT

Tampereen ammattikorkeakoulu
Tampere University of Applied Sciences
Degree Programme in Paper, Textile and Chemical Engineering
Chemical Engineering

HEIDARI RULIS:
Synthesis, Characterization and Application of Hydrophobic Zeolites

Bachelor's thesis 54 pages, appendices 7 pages
December 2016

The aim of the thesis was to design and synthesize a type of zeolite with the characteristics of hydrophobicity, high porosity, and proper pore size, which can be used for high-performance adsorption of ethanol from aqueous solution. In addition, the aim was to synthesize hydrophobic microporous zeolites including theoretic and experimental content.

The experiment was carried out using hydroxide basic system and hydrogen fluoride neutral based on hydrothermal methods. Pure silica zeolites with fewer defects are expected to be highly hydrophobic, highly porous and to have uniform pore size. A series of pure silica zeolites with different porosity were designed and synthesized and their adsorption performance of ethanol from dilute aqueous solution was tested. The characterization of zeolite was performed by powder X-ray diffraction measurement, scanning electronic microscope for possessing cubic morphology and uniform crystal size and nitrogen adsorption-desorption analysis for evaluating porosity. The adsorption of ethanol from aqueous solution was done by using a sealed flask containing a known amount of ethanol–water mixture. The adsorbed amounts of ethanol were tested by using gas chromatography.

As a result of experiment, the powder X-ray diffraction patterns indicated that every samples had the framework type MFI structure with crystallization and high purity. Scanning electronic microscope (SEM) images showed the possessed cubic of morphology and uniform crystal size between 1.0–5.0 μm and 100–200 nm differing with different images and samples. Nitrogen adsorption-desorption isotherms demonstrated that the materials were type-I adsorption isotherms (Langmuir isotherm or type-1 isotherm describes a rapid rise approaching a maximum value asymptotically as the vapour pressure increases in the adsorption isotherms diagram) indicating microporous materials. Finally, adsorption testing showed that the performance of hydrophobic zeolites was better than ordinary zeolites. Hydrophobic zeolites can be used, e.g., in removal of organic molecules, air pollution and adsorption of alcohol from water, which is a physical adsorption by van der Waals forces. The adsorption ability is based on the adsorption surface. Zeolite has a potential application in bio-ethanol separation process, for instance, processing bio-ethanol from biomass via fermentation.

Key words: Zeolites, hydrophobic, MFI, adsorption, bioethanol

CONTENTS

ABBREVIATIONS AND TERMS

BET	Brunauer-Emmett-Teller, BET surface area, which is a physical adsorption of gas molecules on a solid surface.
CAS	Chemical Abstracts Service
Co. Ltd.	Company limited
EMT	Hexagonal polymorph of faujasite-type zeolite
FCC	Fluid catalytic cracking
FID	Flame ionization detector
GC	Gas chromatography
GLC	Gas liquid chromatography
HF	Hydrogen fluoride
Hydrothermal synthesis	A method that is used to crystallize chemical compounds from an aqueous solution in a sealed container at high temperature and vapour pressure.
ID	Inner detector of the capillary column
Invertase	an enzyme, which is used as catalyst to hydrolyse sucrose
LTA	Linde Type A, zeolite A
MFI	Framework type MFI structure
PAA	Poly-acrylic acid
PXRD	Powder X-ray Diffraction
SDAs	Structure Directing Agents
SEM	Scanning Electronic Microscopy
SOD	Sodalite zeolite
Solvothermal synthesis	A method of crystallizing chemical compounds from a non-aqueous solution in an autoclave at high temperature and pressure.
TEOS	Tetraethyl Ortho-silicate
TPAOH	Tetrapropylammonium hydroxide
Type-1	A type of adsorption isotherms, also called Langmuir isotherm, which characterizes microporous adsorbents.
ZSM-5	Zeolite Socony Mobil-5

1 INTRODUCTION

In this thesis, the aim was to design and synthesize different kind of zeolites with the characteristics of hydrophobicity, high porosity, and proper pore size, which can be used for high-performance adsorption of ethanol from aqueous solution. This has a potential application in bio-ethanol separation process, for instance, processing bio-ethanol from biomass via fermentation.

The first natural zeolite was discovered more than 200 years ago, after long-term practical applications. At the same times, the microporous properties of zeolites such as reversible water-adsorption were recognized. Zeolites are crystalline microporous aluminosilicates, which consist of tetrahedral units producing open framework structures, cavities and channels molecular dimensions. Silicon-oxygen tetrahedral in quartz (SiO_2) become electrically neutral connecting to each other in a three-dimensional network. Zeolites have the regular and uniform porous structures. The porosity structure can be described by using several parameters such as pore size and shape, channel dimensionality and direction, composition and features of channel walls. There are more than 40 different types of natural zeolites. Chabazite, clinoptilolite and mordenite are the most famous and used natural zeolites. During the past centuries, scientists have found by far 229 synthetic zeolites including zeolite A, X and Y.

Zeolites have had a major impact on science and technology such as catalytic in industrial and medical processes. Zeolites have been used in the purification and separation of mixture gas by selective adsorption. The components of zeolite on a micro- or mesoporous solid adsorbent have a major unit operation in the chemical, electronic, environmental, medical and petrochemical gas industries. The most important application uses of zeolites are in the agriculture, purification of waste water, medicine, separation of gases. They are also used as catalysts in petroleum refining, petrochemical, and in the field of cracking, hydrocracking, isomerization, alkylation and reformation reactions.

Bioethanol is a type of sustainable biofuel, which has attracted great attention all over the world. Recovery of ethanol from fermentation mixture requires significant energy by using traditional distillation process. The selective adsorption method is proven a less energy-intensive technique.

2 ZEOLITES

This part deals with the applications, history, properties and especially structures of zeolites, such as microporous channels, 3-dimensional channel systems, and various cage structures and also natural and synthetic type of zeolites. Knowing the proper pore size and crystallinity of zeolites is really important when it comes to the experimental of synthetic zeolites. Zeolites are microporous aluminosilicate minerals, which consist of frameworks, component elements, and channel structures with different sizes, pore dimensions, pore shapes and molecular arrangement. Microporous compounds can be crystallized by hydrothermal and solvothermal synthetic methods. Zeolites usually contain guest species like organic molecules or metal complexes in their structures. For example, structure-directing agent (SDAs) or organic residues interacting with zeolite frameworks via hydrogen bonds or van der Waals (attractions between a molecule and its neighbouring molecule). The guest molecules and residues are needed to be removed from the microporous compounds, in order to extend the surface properties of zeolites. The guest molecules from the microporous frameworks can be removed with high-temperature (550 ℃ in air) calcination by oxidizing and decomposing the organic molecules. (Chen, Huo, Pang, Xu & Yu 2007, 345–346)

2.1 History of zeolites

Natural zeolites were created from the interaction between ash and volcanic rock with underground water. They were exposed to high temperatures and pressures and this established the physical and chemical changes over millions of years ago. The porous natures of zeolite have been crystallized and developed during the years in the lake and marine basins. Swedish mineralogist Axel Fredrik Cronstedt (1722–1765) uncovered a natural zeolite in 1765 (Inglezakis & Loizidou 2012, 3). The term “zeolite” comes from the Greek word standing for “boiling stone”, because of its producing loads of steams from water when heated that had been adsorbed by the material. Nevertheless, zeolites were identified as a mineral group exactly 260 years ago. The discovery timeline of some important natural zeolites are listed in the following table (Table 1). (Inglezakis & Loizidou 2012, 3–6; Wang 2009, 23–25; Woodford 2016)

Table 1. Discovery timeline of some natural zeolites (Inglezakis & Loizidou 2012, 3–6)

Zeolite	**Year**
Stilbite	1756
Natrolite	1758
Chabazite	1772
Analcime	1784
Heulandite	1801
Philipsite	1824
Faujasite	1842
Mordenite	1864
Clinoptilolite	1890
Erionite	1890
Ferrierite	1918

18 naturally occurring zeolites were discovered by 1825 and 7 more during the 19th century and another 25 in the 20th century. Huge beds of rich zeolite sediments formed by the variation of volcanic ash in the lake and marine waters, were explored in the Western United States of America and in the other parts of the world in the late 1950s. Zeolites were also discovered in marine tuffs in Italy and Japan. From then on, similar deposits have been found around the world, such as in Cuba, Hungry and New Zealand. During the past 200 years, the Scientists have discovered over forty different types of natural zeolites. (Inglezakis & Loizidou 2012, 3–6; Wang 2009, 23–25; Woodford 2016)

2.2 Natural and synthetic zeolites

Zeolites are the largest group of the minerals among the silicates, which perform more than 40 naturally occurring species. Naturally, many of zeolites occur as minerals, e.g., in sedimentary rocks, and are widely mined in many parts of the world. The most known natural zeolites are analcime, chabazite, clinoptilolite, erionite, ferrierite, heulandite, laumontite, mordenite and philipsite. The most mined natural zeolites are chabazite and clinoptilolite. Different types of zeolites have a different kind of channels and cavities. Some important of crystal structure of zeolites are given in the following figure (Figure 1). (Auerbach, Carrado & Dutta 2003, 2–5; Inglezakis & Loizidou 2012, 3–6; Leavens 2016)

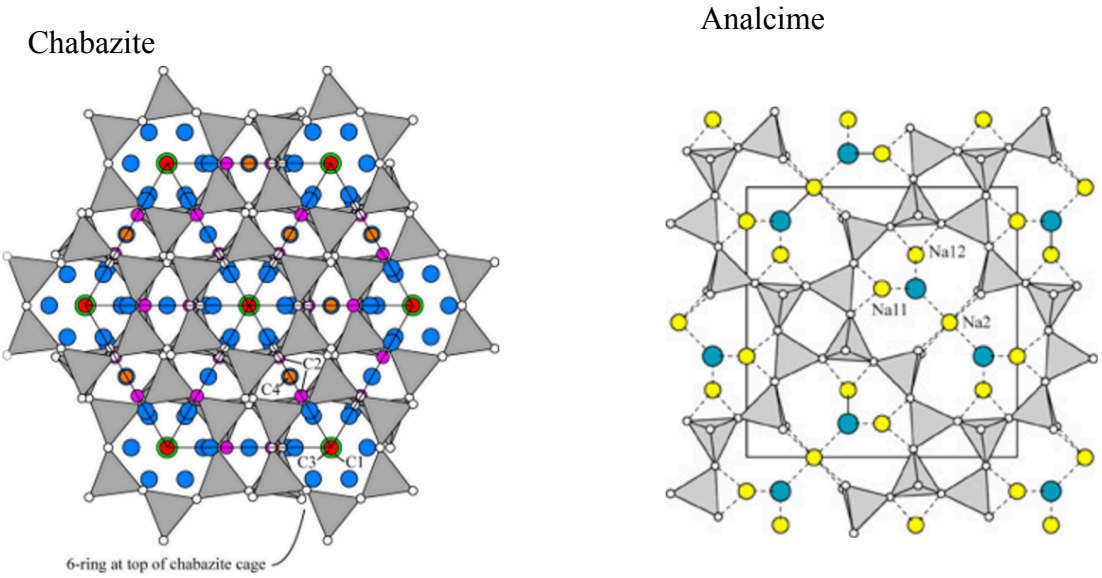

Figure 1. Structure of chabazite and nalcime: Cations in colours, H_2O molecules in blue (The commission on natural zeolites 2005)

There are about 229 synthesized zeolites and the most common are zeolite A, X, Y and ZMS-5. Synthesis of zeolites was first carried out through mimicking of the geothermal conditions for natural zeolite formation at the end of 19th century. In the late 1940s, scientists started doing research on massive synthesis of zeolites. Plentiful of natural zeolites were found later in the sedimentary rocks near the surface of the earth. Low-silica zeolite was the first zeolite to be synthetized using hydrothermal synthesis technique at temperature of around 25–100 ℃ in 1940s. Zeolite A and X began to be produced industrially by the end of 1950s. Synthetic zeolite market started to materialize in 1960s, when their large-scale use for catalytic cracking in petroleum refining began. Since then, researchers have synthesized 229 zeolites in an effort to discover more efficient catalysts because of their great value in petroleum industries. The demand point of synthesis zeolites began to spike in the 1970s, when they replaced phosphate compounds in laundry detergent powders. The Companies in the United Stated of America, such as Linde, UCC, Mobil, and Exxon, mimicked the formation of natural zeolites and produced a series of synthesized zeolites with an intermediate Si/Al ratios including NaY, mordenite, zeolite L, eronite, chabazite and clinoptilolite. These kind of zeolites are widely used in the field of gas purification and separation, catalytic process of petroleum refining, petro-chemistry and ion exchange. (Chen et al. 2007, 1–3; Virta n.d.)

2.3 Properties and structure of zeolites

Zeolites are hydrated crystalline aluminosilicate minerals, which are made from inter-linked tetrahedral of alumina (AlO_4) and silica (SiO_4). They also consist of the chemical elements aluminium, oxygen and silicon, included alkali or alkaline-earth metals and the water molecules are trapped in the gaps between them. $M_{2/n}O \cdot Al_2O_3 \cdot xSiO_2 \cdot yH_2O$ is the general formula of crystalline aluminosilicates, where n is the valence of the cation, M, x and y may vary from 2 to infinite atomic units and Si/Al ratio (Gilson & Guisnet 2002, 3). Zeolites are inorganic microporous minerals, which are formed with three-dimensional crystal structures. They have many large open pores cage-like cavities and are arranged regularly and roughly in the same small-size molecules (Figure 2). (Inglezakis & Loizidou 2012, 3–6)

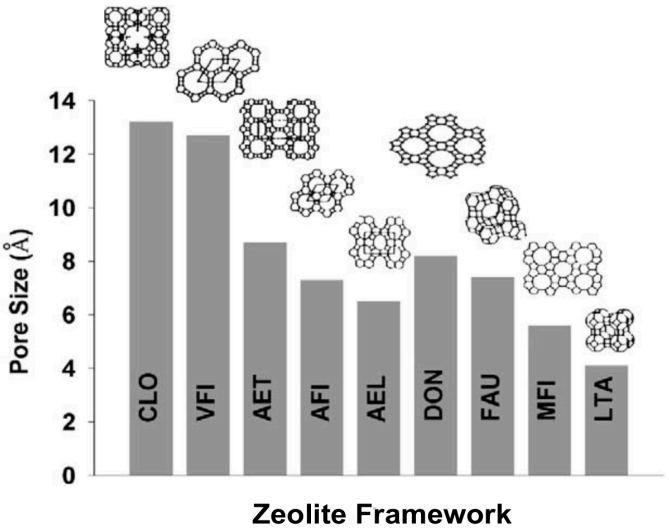

Figure 2. Comparison of pore size of different framework structures (Auerbach et al. 2003, 2)

Zeolites can be paralleled to a sponge, where each molecule can be absorbed in if they can fit through the microscopic holes of zeolites. Too large molecules are not able to go through the gap. Zeolites have the ability to exchange inherent cations for other cations on a basic of ion selectivity. They also have the ability to absorb molecules, gases and vapours, and to absorb/desorb water without any chemical or physical exchange in the zeolites matrix. Among the other things, carbon dioxide, sulphur dioxide, oxygen, nitrogen dioxide, water molecules and other tiny molecules can be adsorbed through the

microscopic holes. The tetrahedral of silicon-oxygen are electrically neutral connecting together in a three-dimensional network as in quartz, SiO_2 (Anderson & Rocha 1996, 35). Positively charged aluminium (Al^{3+}) makes the framework negatively charged in the silica framework, which requires the presence of extra-framework cations to keep the structure of overall framework neutral. The extra-framework contains alkali or earth-alkaline metals such as K^+, Na^+ and Ca^{2+}, which are generally changeable (Figure 3). The framework consists of open cavities in the form of channels and the cages are often filled by H_2O molecules. The channels are sufficient big to let the passage of guest molecules. The following three components can be described the composition of zeolite (Anderson & Rocha 1996, 35–36; Inglezakis & Loizidou 2012, 3–6):

$$M_{n/m}^{m+} \cdot [Si_{1-n}Al_nO_2] \cdot nH_2O$$

extra-framework cations · framework · sorbed phase

Whereas, M is an extra-framework exchangeable cation of valence *m* and *n* is the number of molecules of water, silicon and aluminium and bracketed term submits the framework composition.

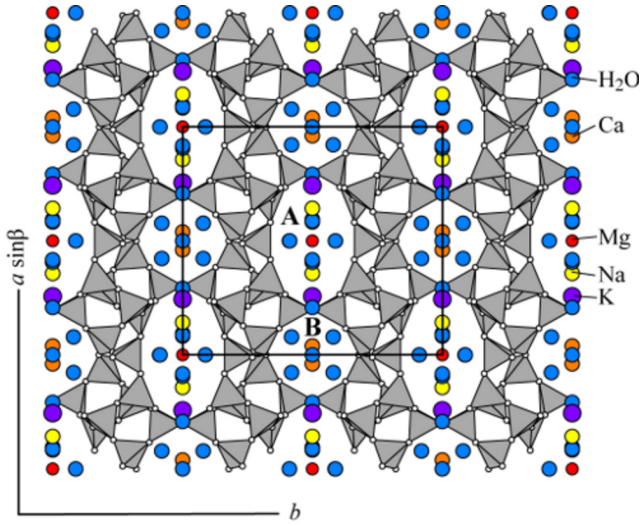

Figure 3. The crystal structure of clinoptilolite-Na with cation positions (The commission on natural zeolites 2005)

Zeolites come with a natural porosity, since they have a crystal structure including pore sizes ("window") and cage-like cavities. In general, natural zeolites are hydrophilic (have an affinity to water) because of their limited pore sizes (Inglezakis & Loizidou 2012, 25). Some of the synthetic zeolites are hydrophobic, which are considered as an adsorbent. Synthetic zeolites can adsorb water and organic molecules similar to their sizes. Diffusion of molecules in the zeolite pores involve adsorption and catalytic processes, where those with minimum of 8 tetrahedral (8T) atom apertures are allowed to diffuse into zeolite pores (Figure 4). Zeolites can be divided into three categories according to their pore sizes:

- small pore zeolites, which have eight membered–ring pore apertures with 8T atoms and having free diameters of 0.30–0.45 nm,
- medium pore zeolites having ten membered-ring apertures from 0.45–0.60 nm in free diameter,
- and lastly, large pore zeolites, which have 12 membered-ring apertures in 0.60–0.8 nm diameter (Gilson & Guisnet 2002, 4).

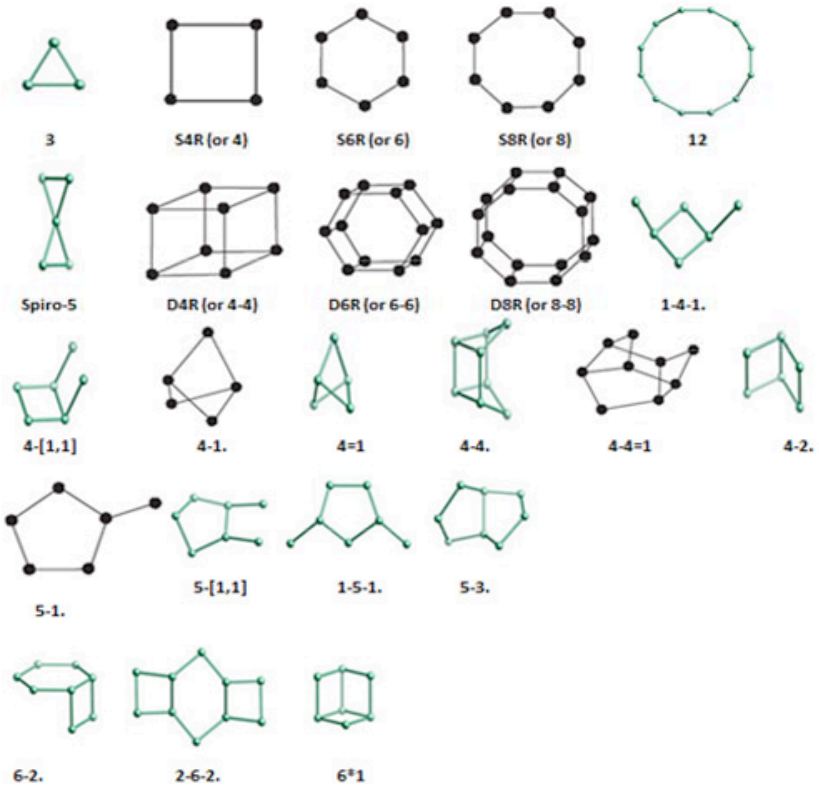

Figure 4. Secondary building units in zeolites (Anger & Ulmanu 2012, 70–72)

The most common produced synthetic zeolites are A, X, Y, L (zeolite with the low form of silica) and ZSM-5 (zeolite with the high silica form, Figure 6). NaA, NaX and NaY are the low silica form of synthetic zeolites, which are widely used in industry as ion-exchangers, adsorbents and catalysts. Many of zeolite structures are based on sodalite unit or β-cage consisting of 24 alumina $[AlO_4]^{5-}$ and silica $[SiO_4]^{4-}$ tetrahedral linked together. The rings contain 4 and 6 Si / Al atoms, which are linked together forming a truncated octahedron (limited numbers of digits). β-cage is found in sodalite (SOD), LTA (Linde Type A), faujasite and EMT (Figure 5). (Anderson & Rocha 1996, 10; Anuwattana & Khummongkol 2009, 470–472)

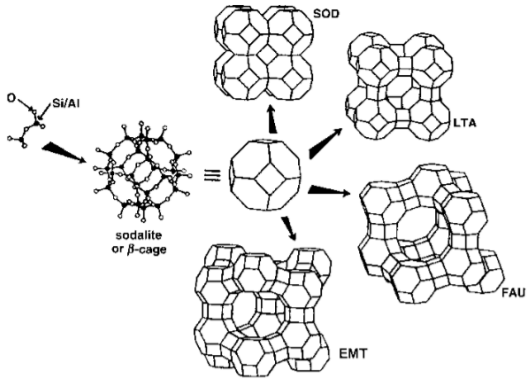

Figure 5. Many zeolite structures are based on sodalite unit, including SOD, LTA, FAU and EM (Anderson & Rocha. 1996, 10)

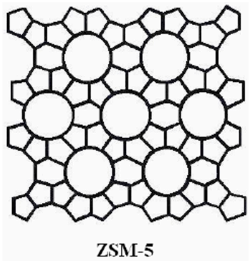

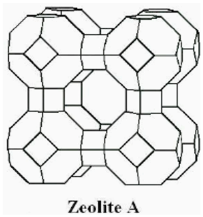

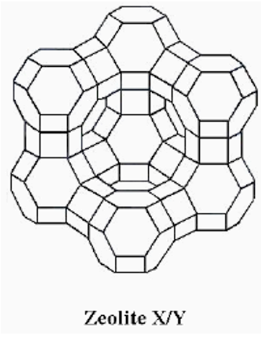

Figure 6. Structures of some synthetic zeolites (Anuwattana & Khummongkol 2009, 470–472)

3 BIOETHANOL

Bioethanol is a renewable and biodegradable biofuel, which is commonly produced from ethanol. Chapter 3 deals with the properties and application of ethanol, structures of carbohydrates, the raw materials of bioethanol and its productions. Ethanol adsorption has an important and wide range of application in synthesis of zeolites.

3.1 Ethanol

The differences between biodiesel and bioethanol are in both conversion technology and raw materials. The basic conventional chemical technology process is used to transform oilseeds and grans into biodiesel and bioethanol. Biodiesel are made from rapeseed, green canola seed, sunflower seed, palm kernel, soybean seed, peanut seed et cetera. Bio-alcohol is ethanol, which is made from plant-based raw materials such as starch, cellulose or sugar fuel plants by sugar fermentation process. It can also be produced by the chemical process of reacting ethylene with steam. Ethanol also called ethyl alcohol is a clear, colourless, volatile and flammable liquid with a characteristic odour at room temperature. It is also biodegradable and has low environmental pollutant. Ethanol consists of two carbons and five hydrogen molecules and has an OH (hydroxyl) group attached to a saturated carbon atom (Figure 7). (Campelo, Clark & Luque 2011, 60–70; NutrientsReview 2016; Bioethanol for transportation 2016)

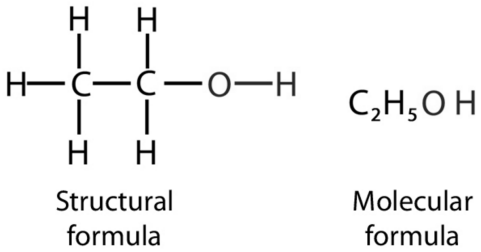

Figure 7. Molecular and structure formula of ethanol (NutrientsReview 2016)

3.2 Production of bioethanol

Bioethanol is produced from biomass by two basic steps, fermentation and biological processes. These basic steps have been used to produced wine from sugar for decades. Ethanol is the most common renewable fuel, which derived from corn grain (starch) and sugar cane (sucrose). Unlike biomass, which is composed of cellulose (4–50 %), hemicellulose (35–35 %) and lignin (15–25 %), in corn grain the major carbohydrate is starch. Enzymatic liquefaction and saccharification (hydrolysis of sugars) are used to produced clean glucose from starch or cellulose, these follows distillation of alcohol producing higher concentration of alcohol. In general, the feedstocks of production of bioethanol are energy crops, which includes sugar cane, corn, maize, sugar beet and wheat. Brazil is the major global producer of bioethanol producing 50 % of the world fuel ethanol from sugar cane juice and molasses and the country replies 25 % of all sugar cane production worldwide. On the other hand, United States of America is the lead producer of fuel ethanol using corn. (Bioethanol for transportation; Campelo et al. 2011, 60–70; Emptage, Zhao & Gray 2006, 141–142)

A storage compound of starch consists of glucose linked via α-1,4 (Figure 8) and α-1,6 glycosidic linkages (amylose and amylopectin). A structural compound of cellulose is composed of exclusively of glucose linked via β-1,4 glyosidic bonds. Cellulose is highly crystalline, compact and making it very resistant to biological attack because of the β-1,4 linkages. (Emptage et al. 2006, 141–142)

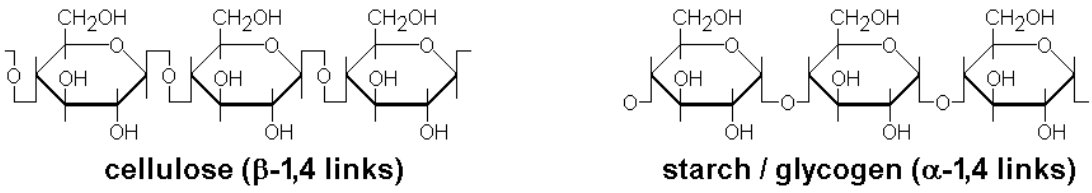

Figure 8. Comparison of cellulose and starch structure formula (Illingworth n.d)

Lignocellulosic biomass consists of hemicellulose, lignin and cellulose. Fuel ethanol production from lignocellulosic biomass can be done in five main steps, which is included biomass pre-treatment, cellulose hydrolysis, fermentation of hexoses, separation and effluent treatment. Sugar from cane and beet are the main feedstock for ethanol

production. Producing ethanol from biomass, it is needed to be pre-treated with acids or enzymes to reduce the size of the feedstock and to open up the plant structure. Cellulose and hemicellulose are hydrolysed by enzymes or dilute acids sucrose sugar. After that, sucrose is converted into fructose and glucose (bio-alcohol) by fermentation process (Equation 1). The lignin in the biomass is used as a biofuel for ethanol production plants boilers. Extracting sugars from biomass can be done in three methods, including concentrated acid hydrolysis, dilute acid hydrolysis and enzymatic hydrolysis. (Campelo et al. 2011, 71-73; Bioethanol for transportation 2016)

1 Production of ethanol from sucrose (Campelo et al. 2011, 5):

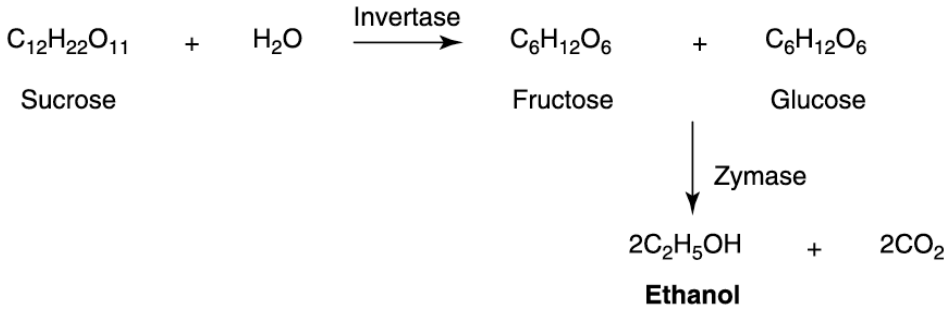

Pre-treatment, which is included physical, chemical and biological treatment to break down the matrix such as hemicellulose, lignin and cellulose from each other by adding 70–77 % sulphuric acid is used in the biomass (10 % moisture content). After that, dilute (0,7 %) sulphuric acid (at 190 °C) is used to hydrolyse the biomass to sucrose. To hydrolyse the biomass by acid, the enzymes can also be used to break down the biomass into small matrixes. Nevertheless, this process is in the stages of development and expensive.

Biomass can also be process into ethanol by wet and dry milling process. To soften and break down the proteins easily, the corn kernel is put into warm water in the wet milling process. After that the corn is milled to produce fibre, germ and starch products. In this process, extracted germ is centrifuged and saccharificated to produce wet cake and this process is commonly used in the factories. In the dry milling process, the corn kernel is broken down into fine particles with the hammer mill process to create the powder product that includes corn germ, starch and fibre. The product is hydrolysed to produce sugar solution by using enzymes or a dilute acid. Fermentation of sugar is the last step of producing of bioethanol. First yeast, which contains an enzyme called invertase

(Equation 2) is added to solution and heated. Invertase is a catalyst, which helps to convert the sucrose sugars into fructose and glucose. (Bioethanol for transportation 2016)

2 Chemical reaction of sugar fermentation process:

$$\underset{\text{sucrose}}{C_{12}H_{22}O_{11}} + \underset{\text{water}}{H_2O} \xrightarrow[\text{catalyst}]{\text{invertase}} \underset{\text{glucose}}{C_6H_{12}O_6} + \underset{\text{fructose}}{C_6H_{12}O_6}$$

The glucose and fructose sugars react with another enzyme called zymase containing in the yeast to produce ethanol and carbon dioxide (Equation 3). Produced ethanol contains a lot of water, which should be removed by using distillation process. The distillation process carried out by boiling water and ethanol mixture. The boiling point (100 °C) of water is higher than ethanol (78.3 °C), so ethanol starts vapouring before the water and this can be condensed and separated. (Bioethanol for transportation 2016)

3 Synthesis of ethanol is shown below:

$$\underset{\text{glucose/fructose}}{C_6H_{12}O_6} \xrightarrow[\text{catalyst}]{\text{zymase}} \underset{\text{ethanol}}{2 \cdot (C_2H_5OH)} + 2CO_2$$

Bioethanol is a renewable resource, biodegradable, less toxic and it has low greenhouse gas emissions over fossil fuels. Fuel or energy crops are the main resources of sugar, which is required to produce ethanol. Bioethanol is used as a biofuel for transportation applications or an additive in many chemical industries. (Bioethanol for transportation 2016; Campelo et al. 2011, 60–70; NutrientsReview 2016)

4 ADSORPTION ISOTHERMS

In this section, the different types of adsorption isotherms are explained. The process of adsorption is important in the studies through graphs, which is called adsorption isotherm. Surface area is area, where a solid material interacts with its surroundings, such as liquid and gases.

There are two types of surface adsorption mechanisms: physical adsorption (physisorption) and chemical adsorption (chemisorption). Physical adsorption is a process, which is caused by weak van der Waals forces (attraction and repulsions forces between molecules, atoms, intermolecular forces and surfaces). The ability of the adsorption is based on the adsorption surface area and it takes small amounts of energy to remove physical species from a solid surface. Physical adsorption provides information about surface area and pore size of the materials. On the other hand, chemical adsorption is a process, which is caused by chemical valence forces including a chemical reaction (transfer of electrons) between the surface and the adsorbate (a substance, which has ability to be adsorbed, surrounding fluid). Chemical adsorption is a monolayer adsorption, which can be used for characterization of catalyst surfaces and heterogeneous catalysis of chemical reactions. Both physical adsorption and chemical adsorption are usually studied through graphs called adsorption isotherm (Figure 9). (Naderi 2005, 585–589)

There are several experimental adsorption isotherms, which can be discerned depending on the physical and chemical conditions of the interactions. Five types of major classifications adsorption isotherms (Figure 9c-g) are commonly observed, which were classified by Brunauer, Deming, Deming and Teller (BDDT). Nowadays, The BDDT is an important classification of gas adsorption isotherms. The Langmuir equation is used to model monolayer formations and BET theorem for using multilayers. Type-1 isotherm is characterized by the Langmuir isotherm in the BDDT classification. Type-1 isotherm describes a rapid rise approaching a maximum value asymptotically as the vapour pressure increases in the adsorption isotherms diagram. This indicates the amount of the adsorbed molecules at the maximum of surface area interacting with the adsorbent. The Langmuir isotherm is the completion of monolayer adsorption, which behaviour obeys for gases, porous and microporous structures materials. (Fletcher 2008; Naderi 2005, 585–589)

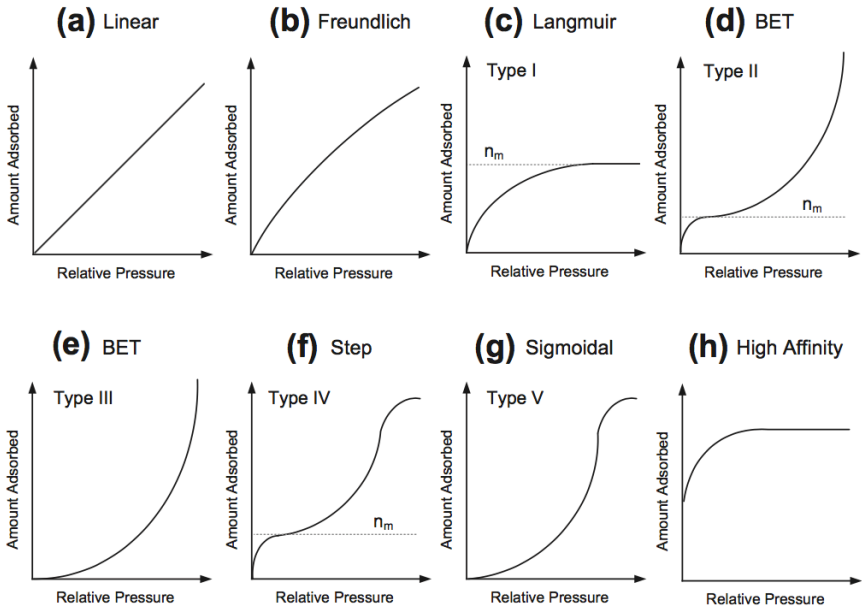

Figure 9. Schematic diagrams of eight adsorption isotherms (Naderi 2015, 588)

Type II BET (Brunauer-Emmett-Teller) isotherm apply to reversible and unrestricted multilayer physical adsorption of gas molecules, which can be happened on non-porous or macro-porous solid materials, such alumina. Type III isotherm is used for explaining multilayer adsorption, where the amount of gas adsorbed increases without limit while relative pressure approaches unity. When the gas pressure is low, the graph indicates low adsorption and low gas-solid affinity. The curve of type IV isotherm is similar to type II at lower pressure. This part indicates monolayer formation and the rest of the graph capillary condensation, which follows the saturation of the adsorbent below the saturated vapour pressure. Type V graph is similar to type IV, except at the beginning of the curve and adsorption is low at the low gas pressures. (Fletcher 2008; Naderi 2005, 585–589)

5 APPLICATION

Zeolites have the most interesting physical and chemical properties of minerals for researching. Zeolites are used in agriculture, purification of waste water, medicine, separation of gases and catalysis due to their cage-like structures and excellent adsorbing properties. This part deals with the few applications of zeolites, such as ion exchange, catalysis and selective adsorption. Selective adsorption is the most essential application in adsorbing materials when it comes to the shape-selective properties of zeolites.

5.1 Ion exchange

Zeolites are classified as framework of aluminosilicate, which consist of either negatively charged tetrahedral alumina (AlO_4) or silica (SiO_4) making the trivalent state of Al. The whole charge of framework is usually neutralised by mono or divalent cations within the framework cavities presenting with water molecules. Zeolites have capability to exchange extra-framework cations and ability to reverse water absorption. Owing to their cage-like structures, zeolites are used in ion exchange as water softeners. There the hard water (with rich amount of calcium and magnesium ions) is pumped through a column filled with sodium containing zeolites. Positively charged calcium (Ca^{2+}) and magnesium ($Mg^{2+)}$ ions will be attracted with negatively charged zeolite molecules in their channels, where sodium ions are replaced by calcium and magnesium ions (Equation 4). When the ion exchanged has been happened, the water will become softer containing large amount of sodium (Figure 10). Zeolites are also used in the laundry and dishwasher detergents, removing radioactive particles from nuclear water, toxic heavy metals cleaning up, odour control and pet litter. (Woodford 2016; Degnan 2000, 349–352)

4 Reaction of calcium ion with sodium zeolite:

$$Na_2Ze + Ca(HCO_3)_2 \rightarrow 2NaHCO_3 + CaZe$$

$$Na_2Ze + CaSO_4 \rightarrow Na_2SO_4 + CaZe$$

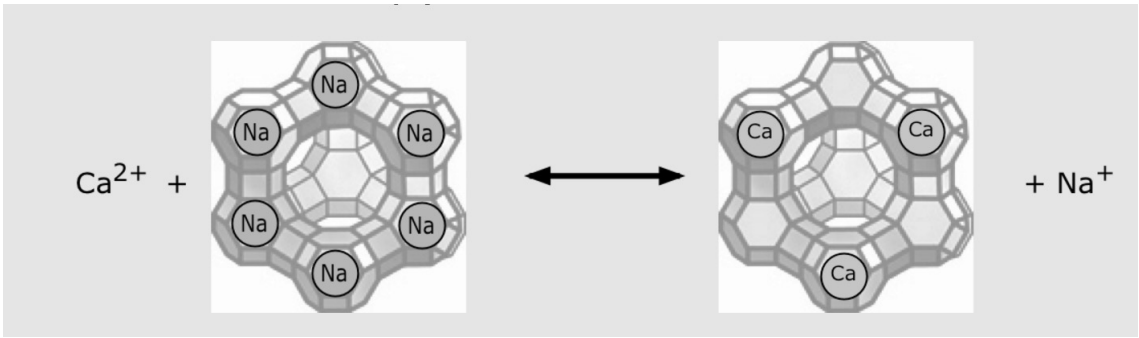

Figure 10. Process of ion exchange: positively charged calcium ion exchange with negatively charged zeolite (Lower 2013)

5.2 Catalysis

Zeolites have been used as catalysts in the industry fields since late 1950s. Zeolite Y, faujasite, mordenite and ZSM-5 are the most used zeolite catalysts in pharmaceutical and petrochemical industry. They are also used as catalyst in catalytic crackers to break hydrocarbon polymer molecules into diesel, gasoline, kerosene, waxes and other by-products of petroleum. After discovering zeolite ZSM-5 in 1967, it led to many essential new processes, such as dewaxing, methanol to gasoline and olefin oligomerization. The majority uses of zeolites are in catalytic cracking and hydrocracking field. On account of the structures, acidity and shape-selectivity of zeolite, it is used as catalysts in chemical synthesis and in organic synthesis. The pores of zeolite are similar to small organic molecules. It has shown the ability to recognize, discriminate and organize to those molecules, which have less than 1 Å pore sizes. Zeolites have also ability to control the catalytic properties and acidity using synthetic and post-synthetic methods.

Fluid catalytic cracking (FCC) is the most used zeolite catalyst. Zeolite Y has been used as a primary zeolitic component in fluid catalytic cracking catalyst for years. Zeolite Y is used in the refining petrochemical field such as catalyst, which provides the greatest and the highest octane with the great degree catalytic stability. It is also used as FCC to improve coke selectivity, higher cracking activity, and greater stability through manipulation of extra-framework aluminium. Extra-framework aluminium can be introduced either by steaming or via ion exchange. Zeolite can also be used as an additive in the refining field such as ZSM-5. A small amount of ZSM-5 is added to FCC unit improving gasoline octane. (Davis & Dartt 1994, 151–156; Degnan 2000, 349–352)

Double-bond isomerization can be catalysed either by basic or acidic zeolites. Basic catalysts are used due to their high selectivity. Aldo Condensation is shown in the following figure (Figure 11) to be catalysed by zeolites in the gas phase reaction between formaldehyde and methyl propionate forming methyl methacrylate. (Davis & Dartt 1994, 156)

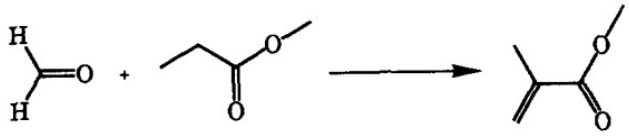

Figure 11. Aldo condensation between formaldehyde and methyl propionate to form methacrylate c

5.3 Adsorption and separation

Zeolites have been used in the purification and separation of mixture gas by selective adsorption. Their components on a micro- or mesoporous solid adsorbent has a major unit operation in the chemical, electronic, environmental, medical and petrochemical gas industries. The most important application uses of zeolite are in the agriculture, purification of waste water, medicine, separation of gases and catalysis. Zeolites have the essential adsorbing properties, which is used in the material processing with chemical (modification of its structure and composition) and physical (thermal and activation) treatments.

Chromatographic process is used to determined adsorption and separation of materials, which ca be happened on the surface of the materials. Therefore, different migration speed of various compounds along the surface of adsorbent are determined. The molecular adsorption is the basis for the shape-selective properties of zeolites. These type properties are used in a wide range of molecular sieving applications to adsorb certain molecules into zeolites. Depending on the size and shape of pores, the precursor compounds are needed to be smaller than the pore diameter in zeolites to diffuse inside the pores. Different types of molecules enter the zeolite channel at the different speeds, e.g., para-xylene purification by zeolites X or Y. (Chen et al. 2007, 604–606; Peskov 2016.)

Adsorption and crystallization are used in the separation and removal of gases and solvents in the petrochemical industries. Zeolites are used in the purifying and sweetening natural gases by removing impurities like carbon dioxide, sulphur, dioxide and water. In addition, high cost synthetic zeolite molecular sieves are used in separation oxygen and nitrogen in pressure swing adsorption column. Nitrogen and methane gas are removed by using the zeolites from coal mines, natural gas reserves and aging gas wells through the pipeline, as well as, in the adsorption process. Sorbent like large pore zeolites and molecular sieves have an equilibrium selectivity. They are used in the gas purification and separation (Picture 1). Natural zeolites can also be used as an adsorbent in treating the hazardous air pollutants and lots of different organic compounds. Coming with different kind of pore sizes, zeolites are used in controlling air pollutants. Large pore zeolites tend to trap a wide variety of larger molecules, such as ammonia, carbon monoxide, chloroform and formaldehyde. (Inglezakis & Loizidou 2012, 26–30)

Picture 1. Samples of zeolites with penny for scale (Virta n.d., edited)

6 EXPERIMENTAL SECTION

This part focuses on the chemicals, equipment, characterization of zeolites, ethanol adsorption testing and actual synthesis of zeolites. The experimental procedure is the most important part in this section, where two types of methods (OH^-- and F^-- system) were used to synthesize the silicalite-1.

6.1 Chemicals

In this experimental procedure, zeolites were successfully synthesized by hydrothermally treatment of the mixture of tetrapropylammonium (TPAOH, 25 %), water (H_2O) and tetraethyl Ortho-silicate (TEOS, 98 %), as well as hydrogen fluoride (HF) if required.

Ethanol also known as ethyl alcohol (C_2H_6O) is an important chemical, which has many applications. It is a volatile liquid prepared by fermentation from carbohydrates, such as sugar and yeasts. Ethyl alcohol is used in many industrial processes, for instance, in the chemical synthesis of esters, organic and cyclic compound chains, detergents, paints, cosmetics, aerosols, perfumes, medicine, food and other chemical as a feedstock. In addition, ethanol is used as a fuel additive and alternative biofuel. Some of the important properties of ethanol is shown in the following table (Table 2). Chemical Abstracts Service (CAS) assigned to identify every chemical substance, including organic and inorganic compounds, minerals, isotopes, alloys and non-structural materials to disclose chemical substance information. The density of ethanol is 0.789 g / ml in the room temperature about 20 ℃, whereas the boiling point 78.5 ℃. (Penoncello, Schroeder & Schroeder 2014; Pubchem 2016.)

Table 2. Properties of ethanol (Pubchem 2016)

Cas-number	64–17–5
Formula	C_2H_6O
Molecular weight	46.07 g / mol
Density	0.789 g / ml (20 ℃)
Boiling point	78.5 ℃

Hydrogen fluoride or hydrofluoric acid (HF) is a colourless gas or a fuming liquid, highly corrosive and extremely toxic chemical compound. It is used in manufacturing of hydrofluoric acid as reagent, catalysts and fluorinating agent. It is also used in making refrigerants, herbicides, high-octane gasoline, aluminium, electrical components, fluorescent light bulbs, pharmaceuticals, plastics and in the refining of uranium and the preparation of many fluorine compounds. Exposed a high amount of HF into nature, it will cause a natural disaster. Skin contact with the hydrogen fluoride, it may cause skin burn and cell damages. Hydrogen fluoride density is about 1.15 g / mole (25 ℃) in a gas phase and its boiling point 19.5 ℃ (Appendix 1). (Facts about hydrogen fluoride 2013 & Pubchem)

Tetraethyl Ortho-silicate (TEOS) also known as ethyl silicate is a chemical compound, which consists of four methyl groups attached to the hypothetical anion SiO_4^{4-}(Figure 12). It is a clear colourless liquid with a faint odour. Tetraethyl Ortho-silicate is used in adhesives and sealant chemicals, crosslinking agent in silicone polymers and as precursor to silicon dioxide in the semi-conductor industry. Tetraethyl silicate is also used in the synthesis of zeolites. As shown in appendix 2, tetraethyl Ortho-silicate has a high boiling point about 170 ℃. The other chemical, which was used in the experiment as a main compound was tetrapropylammonium hydroxide (TPAOH). It is a chemical compound consisting of 12 carbons, 29 hydrogens molecules and one nitrogen and oxygen molecule (Figure 13). TPAOH has a high boiling point about 101 ℃ and density 1.0 g / ml at 20 ℃ (Appendix 3).

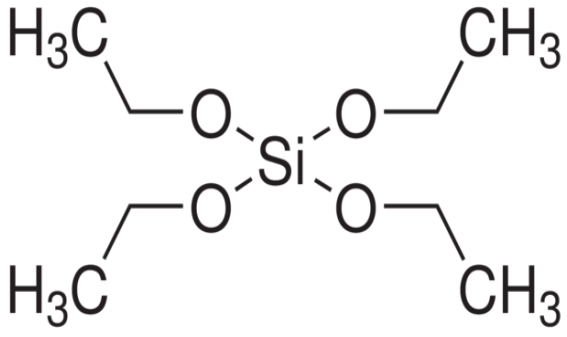

Figure 12. Structure formula of tetraethyl Ortho-silicate (Biomedical 2016)

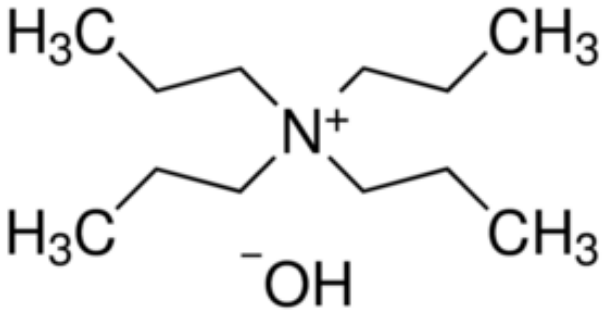

Figure 13. Structure formula of tetrapropylammonium hydroxide (Sigma-Aldrich 2016)

6.2 Equipment

In this experimental section were used the following equipment such as autoclave, centrifuge, electric box resistant furnace, electronic balance, filtration equipment, heating oven, oil bath, stirring equipment, ultrasonic wave, and lab dancer (Appendix 4).

The chemicals were weighted by using an electronic balance (Picture 2). The solutions were stirred on the whirl pool magnetic stirrer (Picture 3). The DF-101S collector-type magnetic stirrer was used as an oil bath (Picture 4) to heat and stir the solution in the collector pot by improving the stirring efficiency and evaporating ethanol from the solution. Autoclave is a pressure cooker that used in the high levels of heat and pressure to sterilize instruments and materials (Picture 5). It destroys harmful organisms and pathogens. Water inside a pressurized container can be heated above the boiling point, which can only be reached 100 ℃ in an open container. Nevertheless, in the pressurized autoclave, the water will reach much higher temperatures. In this experiment, the autoclaves were put into 170 ℃ heating furnace (Picture 6) for 3 days.

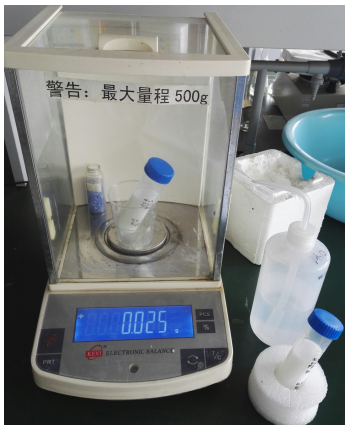

Picture 2. Electronic balance

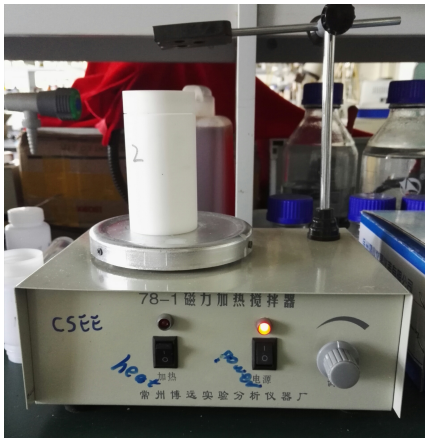

Picture 3. Magnetic stirrer

Picture 4. Oil bath

Picture 5. Autoclave

Picture 6. Heating furnace

Filtration equipment (Picture 7) including circulating water pump was used to filtrate large-sized silicalite-1 from the liquid solution. Lab dancer (Picture 8) and ultrasonic wave mixer (Picture 9) were used to mix the samples in the test tubes. The centrifuge (Picture 10) was used to centrifuged the solutions for 10 minutes at 1.5–2.0 ℃ in 10 000 round per minute. Centrifuge is used to isolate solids in the form of a small pellet from the solution. It is done by spinning closed containers of the mixture very quickly around a fixed and central point. This motion forces the denser material in the suspension against the wall of the container by the centrifugal force generated. In this experiment, the small tubes were utilized to hold the solutions. Electric Box Resistance Furnace (Picture 11) is a closed oven, which is used to calcined the obtained product and remove the organic residues. The product was treated under calcination at 550 ℃ (823 K) for 6 hours.

Gas chromatography is used for quality control, identification, quantitation of compounds and analysing volatile substances in the gas phase (Picture 12). Gas chromatography technique consists of an injection port, a capillary column, carrier gas flow control equipment, ovens and heaters for maintaining temperatures of the injection port and column, a detector and an integrator chart recorder. It requires a mobile and a stationary phase. The components of a sample are dissolved in a solvent and vaporized to separate the analyses by distributing the sample between the phase. Separating the compounds in the gas-liquid chromatography (GLC), a solution sample containing organic compounds of interest is injected into the sample port to vaporize. Injected vaporized samples carried by an inert gas containing usually helium or nitrogen. Inserted gas goes through a glass column packed with liquid coated silica and the less soluble materials goes faster through the column than soluble. Each compound in the sample will spend a different amount of time on the column after it has been injected. The measured time for the inserted compound through a chromatography column is called retention time. (Thet K. & Woo N. 2013)

Image 7. Filtration equipment

Image 8. Lab dancer

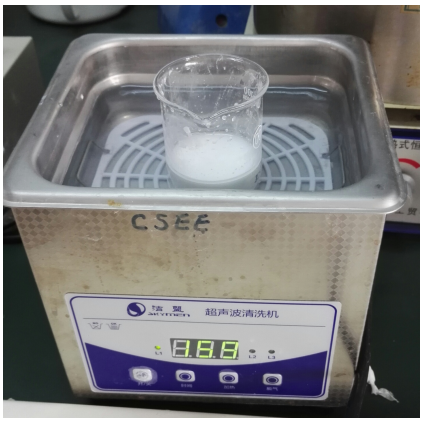

Picture 9. Ultrasonic wave mixer

Picture 10. Centrifuge

Picture 11. Electronic box resistance furnace

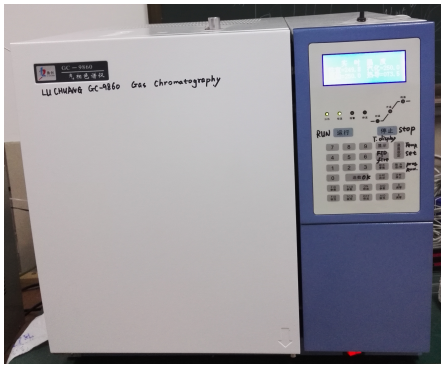

12. Gas chromatography

6.3 Experimental procedure

In this experimental section, each experiment part was designed to synthesize zeolite individually. The experiments were done with two different systems. Synthesis of Nano-sized silicalite-1 (sample A) and synthesis of micro-sized silicalite-1 (sample B) were synthesized by using the hydroxide basic method. Synthesized of large-sized silicalite-1 (sample C) and synthesized of small-sized silicalite-1 (sample D) with hydrogen fluoride based on neutral system. Chemical reagents (Appendix 6) included tetraethyl Ortho-silicate (TEOS), tetrapropylammonium hydroxide (TPAOH) and hydrogen fluoride (HF) were utilized in the experiment. The chemicals that were used in the different experiments are listed in the following table (Table 3). In addition, the most important times of devices, such as the times of heating furnace and electronic box resistance furnace are listed in the Table 4.

Table 3. Design of the experiment

Samples	Name	System	TPAOH 25 % (ml)	H_2O (ml)	TEOS 98 % (ml)	HF 40 % (ml)
A	nano-sized silicalite-1	hydroxide (OH^-)	27	30	16.5	
B	micro-sized silicalite-1	hydroxide (OH^-)	27	30	16.5	
C	large-sized silicalite-1	hydrogen fluoride (HF)	27	30	16.5	4.4
D	small-sized silicalite-1	hydrogen fluoride (HF)	27	30	16.5	4.4

Table 4. The temperatures and times of devices

Device	Temperature (°C)	Time (h)
Electronic box resistance furnace	550	6
Heating furnace	170	72
Oil bath	80	4
Magnetic stirrer	-	0.17

6.3.1 Hydroxide basic method

Synthesis of Nano-sized (sample A) and synthesis of micro-sized (sample B) silicalite-1 were prepared by hydroxide basic method. Firstly, tetrapropylammonium hydroxide (TPAOH) was added into a 250 ml plastic bottle followed by the addition of water (H_2O). The mixture was stirred with magnetic stirrer and tetraethyl Ortho-silicate (TEOS) was added under stirring. After that, the resultant solution was weighted to assure the homogenous of the solution and heated in the oil bath to evaporate alcohol generated during the hydrolysis of TEOS. After completely evaporating alcohol, the clear solution was cooled down, weighted again, added distilled water and transferred into 100 ml Teflon-lined stainless steel autoclaves and hydrothermally treated under autogenous pressure and static conditions (Table 4). The suspend silicalite-1 crystal was centrifuged and washed several times with distilled water to assure and reach the pH 6–8, then the sample was dried overnight. Finally, the obtained product was treated under calcination to remove the organic residues.

6.3.2 Fluoride based on neutral system

Synthesized of large-sized silicalite-1 (sample C) and synthesized of small-sized of silicalite-1 (sample D) were synthesized by using fluoride based on neutral system. First, tetrapropylammonium hydroxide (TPAOH) was added into a 250 ml plastic bottle followed by the addition of water (H_2O). The mixture was stirred with magnetic stirrer and TEOS was added under stirring. After that, the resultant solution was weighted to assure the homogenous of the solution and heated in the oil bath to evaporate alcohol generated during the hydrolysis of TEOS. After completely evaporating alcohol, the clear solution was cooled down, weighted again, added distilled water followed by adding 0.12 g of calcined Nano-sized-silicalite-1 (from sample A) as seeds only to synthesis of small-sized slilicalite-1 (sample D). After stirring, the mixture was transferred into 100 ml Teflon-lined stainless steel autoclaves. Then hydrogen fluoride (HF) was dropped into solution carefully under stirring within a few seconds. Subsequently, the autoclave was sealed and hydrothermally treated under autogenous pressure and static conditions. The suspend silicalite-1 crystal was filtrated, centrifuged and washed several times with distilled water to assure and reach the pH 6–8, and the sample was dried overnight. Finally, the obtained product was treated under calcination to remove the organic residues.

6.4 Zeolite characterization

Chemical analyses were carried out by powder X- ray diffraction (PXRD), nitrogen adsorption-desorption (N_2-adsorption-desorption) isotherms and Brunauer-Emmett-Teller (BET, adsorption of gas molecules on a solid surface and serves) and scanning electron microscope (SEM). The item details are listed in the Appendix 5.

6.5 Ethanol adsorption testing

The adsorption of ethanol from aqueous solution was done by using a sealed flask containing a known amount of ethanol-water. First, the zeolites were weighed and added into beaker (50 ml) and then added water and ethanol under stirring (Table 5). The mixtures were done in a four different test tubes for A, B, C and D samples (Table 3). Then the test tubes were equilibrated for different time at room temperature. After that, the solution was taken from the solution (50 ml beaker) and put it into a test tube. In addition, propanol as internal standard and cyclohexanone as a co-solvent were added into test tube mixture. The liquid samples were withdrawn and analysed by a gas chromatography (GC) equipment testing the left ethanol concentration. Gas chromatography was used to analyse the vapouring compounds and to separate the different components of the mixture (Appendix 5). Gas chromatography (GC) consists of capillary column and flame ionization detector (FID-detector). The different strengths of interaction of the compounds with the stationary phase is the principle of separation of the compounds. The longer the compound interacts with the stationary phase the stronger the interaction is and the more times it takes to migrate through the column.

Table 5. Volume of chemical reagents

Samples	Volume (ml)
Ethanol	1
Cyclohexanone	1
H_2O	19
Propanol	0.10
Test tube	1

7 RESULTS

In this section the results of the experiment and comparisons of two different systems are described. In addition, the characterization of zeolite and ethanol concentration testing are explained.

7.1 Characterization of zeolite

The crystallinity of each synthetic zeolites, silicalite-1 is shown in Fig. 14, with powder X-ray diffraction (PXRD) patterns. In the Figure 14, PXRD patterns demonstrate that every samples had the framework type MFI (ZSM-5) structures with crystallized and high purity. The crystallinity and purity of each samples can be seen in the peaks at 7.8; 8.8; 23.0; 23.9 and 24.4 theta degrees. For the crystallinity and purity of each synthetic zeolites a comparison was done between the peaks at 7.8 theta degrees due to their high intensities. The diffraction intensity of micro-sized silicalite-1 (B sample) was higher than Nano-sized silicalite-1 (Figure 14A), which indicates higher crystallinity of micro-sized silicalite-1 in the presence of hydroxide (OH^-) system including hydrophobicity. After adding a small amount of hydrogen fluoride in the synthetic system (Figure 14C), the diffraction intensity substantially increased compered to Nano-sized silicalite-1(Figure 14A). When a small amount of seeds from Nano-sized silicalite-1(A) was added into small-sized silicalite-1(Figure 14D), it caused slightly decrease in the diffraction intensity (Figure 14C-D) compared to B sample. This shows that the peak at 7.8 theta degree in A sample is smaller than sample B, C and D but higher at 23.0 theta degrees. The outline of the PXRD patterns are shown in the Fig. 15.

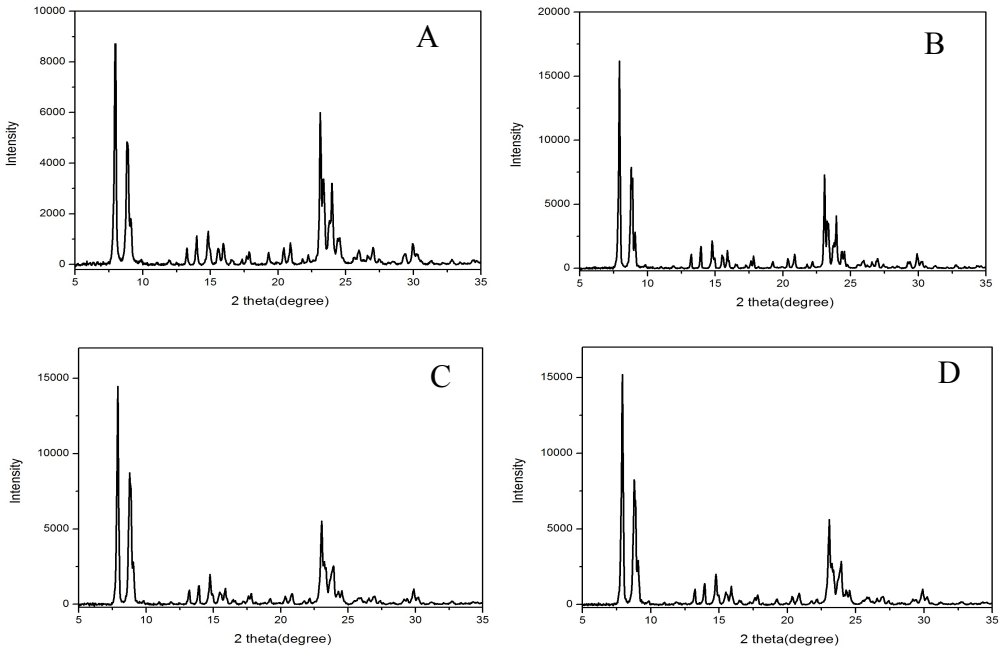

Figure 14. PXRD patterns of final silicalite-1 products (A) Nano-sized silicalite-1, (B) micro-sized silicalite-1, (C) large–sized silicalite-1 and (D) small-sized silicalite-1.

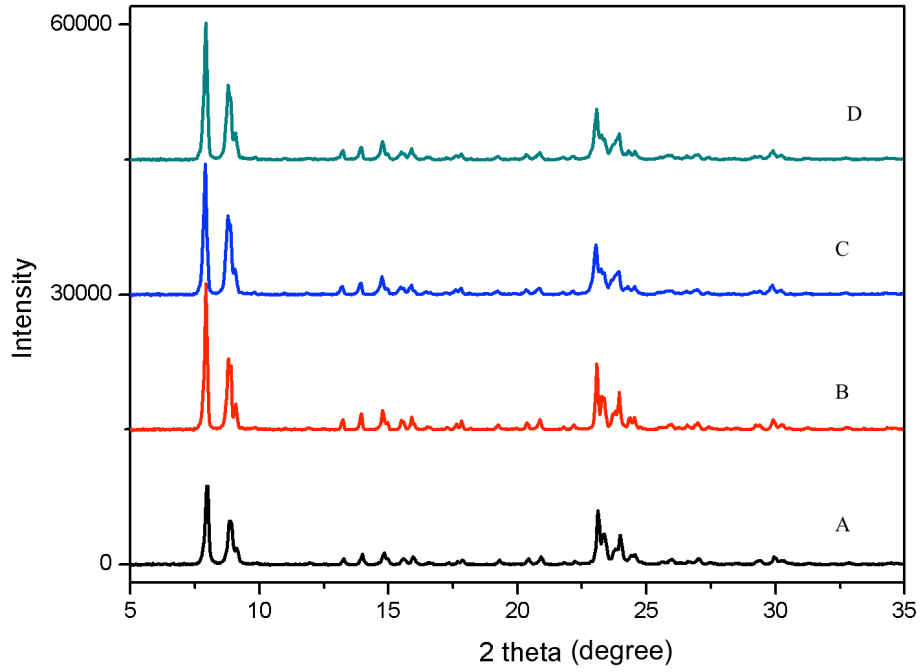

Figure 15. Outline of PXRD patterns of final silicalite-1 products

Scanning electronic microscope (SEM) images show that Nano-sized silicalite-1 (Figure 16A) possessed cubic morphology and uniform crystal sizes of 100–200 nm. Increasing the size of silicalite-1, it will effect on the morphology and crystal size of micro-sized silicalite-1. Micro-sized particles have a plate-like shapes and the uniform crystal sizes are about 1.0 μm, as shown in Fig. 16B. Adding hydrogen fluoride (HF^-) it effected on the crystallization and uniform size of the large-sized silicalite-1 (Figure 16C) and their particles are notably bigger than micro-sized silicalite-1. Large-sized silicalite-1 particles have also the plate-like shapes with uniform sizes about 1.0 x 2.0 μm. After adding hydrogen fluoride and seeds, it did not affect remarkably on its morphology. However, the size of crystal structure reduced and they have no uniform sizes, because of the errors or a small amount of impure in their particles (Figure 16D).

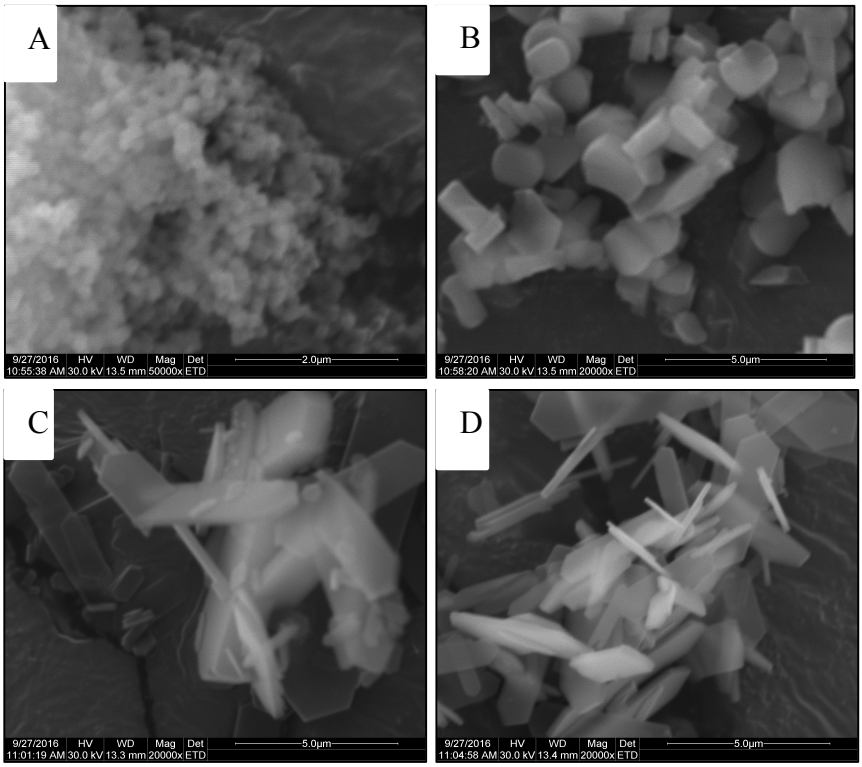

Figure 16. SEM images of final silicalite-1 products (A) Nano-sized silicalite-1, (B) micro-sized silicalite-1, (C) large-sized silicalite-1 and (D) small-sized silicalite-1.

Nitrogen adsorption is a significant method for characterization of porous properties, such as specific surface area, pore volume and pore size (Appendix 7, 8, 9 & 10). Nitrogen adsorption-desorption isotherms (Figure 17) demonstrated that the materials were Type I adsorption isotherms, indicating microporous materials. Type I isotherm is characterized by the Langmuir isotherm in the BDDT classification. It describes a rapid rise approaching a maximum value asymptotically as the vapour pressure increases in the adsorption isotherms diagram. This indicates the amount of the adsorbed molecules at the maximum of surface area interacting with the adsorbent. The Langmuir isotherm is the completion of monolayer adsorption, which behaviour obeys for gases, porous and microporous structure materials. As shown in Figure 17A, the standard relative adsorption curve increases gradually as pressure increases smoothly from 0.1–0.9 p/p_0 and sharply at 0.95–1.0 p/p_0, indicating the Nano-sized particles of this sample. The relative adsorption isotherms for other three samples reaches fast 90 cm^3 /g while the pressure stays at lower p/p_0 (Fig. 17B). The pressure stays constant from 0.35–1.0 p/p_0 in the sample C and D suggesting the big size of these samples.

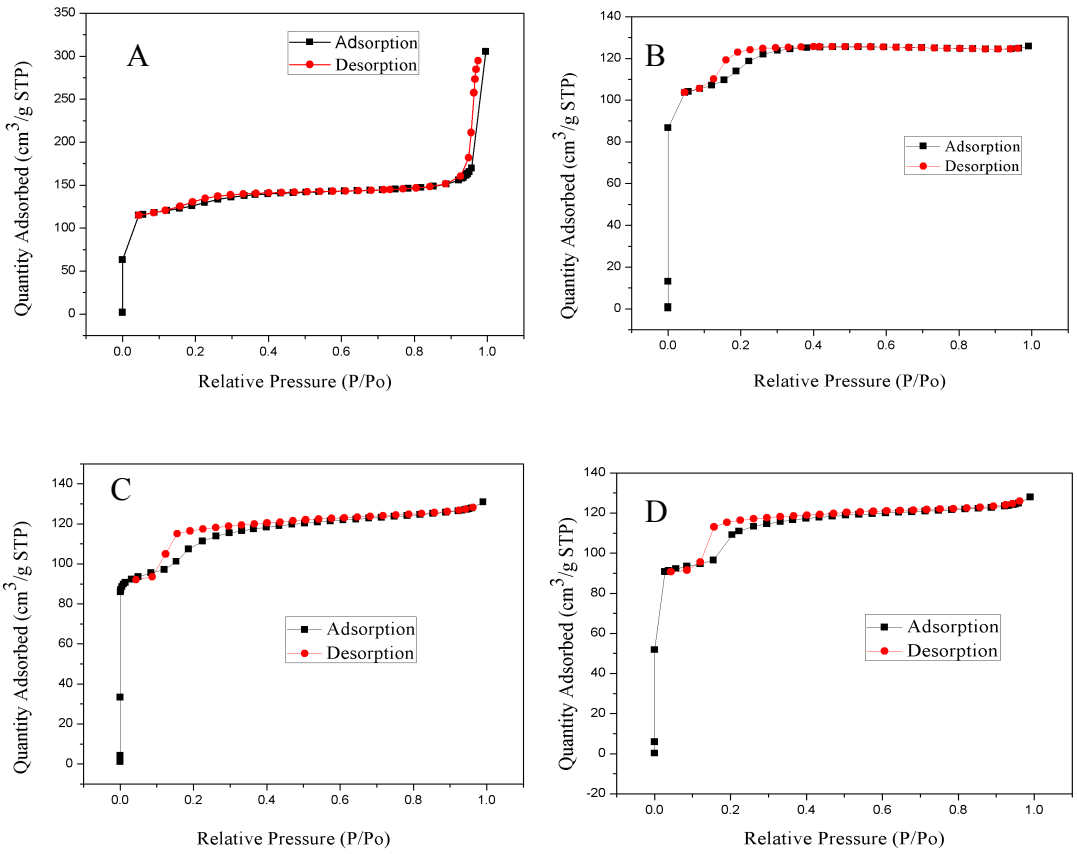

Figure 17. Nitrogen adsorption-desorption isotherms

The surface area of micro-pore volume of the final silicalite-1 products are summarized in table below (Table 6). The sample large-sized silicalite-1 synthesized by hydrogen fluoride based on neutral method containing TPAOH has lower surface area and microporous volume than Nano-sized silicalite-1 synthesized with hydroxide basic system. In the hydroxide basic system, the samples have higher surface area and micro-pore volume than hydrogen fluoride based on neutral system (Table 6). In addition, BET (Brunauer-Emmett-Teller, a physical adsorption of gas molecules on a solid surface) surface areas and micro-pore volumes were measured by the equipment and the results are shown in the Appendixes 7, 8, 9 and 10.

Table 6. Nitrogen adsorption from dilute solution

Sample	Method	Size	BET m^2 / g	Micro-pore volume cm^3 / g
A	OH^-	Nano	428	0.20
B	OH^-	micro	394	0.19
C	HF^-	large	374	0.16
D	HF^-	small	375	0.16

7.2 Ethanol concentration

Ethanol concentration was used to characterise the hydrophobicity of each synthetic zeolite. The adsorption amounts of ethanol concentration in the mixture were tested by gas chromatography equipment, which consists of gas chromatographic column and FID-detector. Vapour pressure and column temperature effects on the separation and different strength of interaction of the compounds with stationary phase. Strong interaction takes longer time for the compounds to interact with stationary phase. In this experiment cyclohexanone was used as a solvent to dissolve the sample because of its low boiling point. As shown in Fig. 18, the temperature of the column starts from 60 °C, which lasts for two minutes, after that, the temperature increases 50 °C / min till 180 °C, which lasts for five minutes.

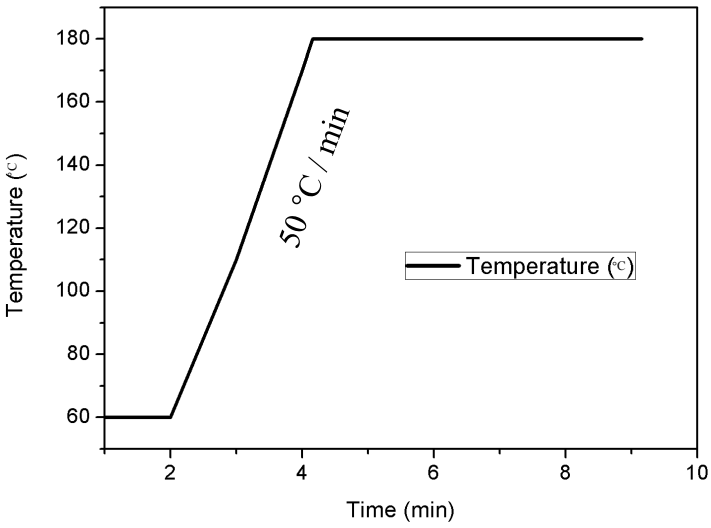

Figure 18. The temperature of column of gas chromatography

Figure 19 represents a standard chromatogram produced by a FID detector. In the standard chromatogram, the x-axis is the time and the y-axis is the absorbance. The retention times and the peak heights are determined from the chromatograms. In these chromatogram first peak represents ethanol peak (1.433 min), the second peak internal standard propanol (1.718 min) and the third (3.622 min) and the longest peak represents the cyclohexanone solvent.

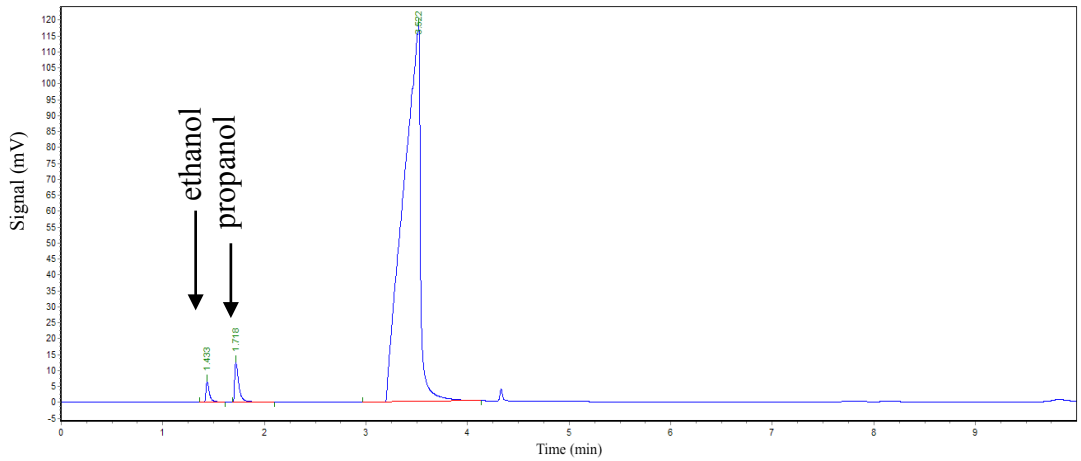

Figure 19. Standard chromatogram of a mixture gases

The calibration equation (5) based on internal standard of propanol was used to get to know the relation between mass and peak area. The known amount of ethanol was prepared and used in analysing of component of the compounds by gas chromatography. The calibration curve or standard curve was used to determine the relationship between the magnitude of a peak for a known amount of analyte in the standard. Injection amount, split ratio, linear choice, temperatures, flows, pressures, detector set points are related to analysing samples. The calibration curve for ethanol adsorption is linear and goes through zero, as shown in Fig. 20, where the slope of the calibration function for propanol is about 1.105. The peak area of the unknown sample can be divided by slope (y / k) to determine the amount of ethanol in the sample. The peak areas of ethanol and internal standard propanol are shown in the following table (7). For the rest of the samples the peak areas of ethanol and propanol are listed in the appendixes 11, 12 and 13.

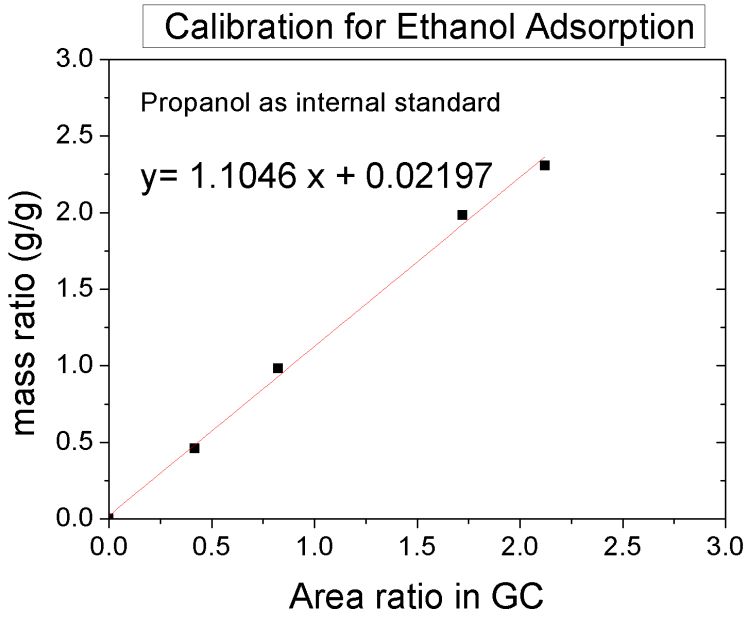

Figure 20. Calibration equation of ethanol adsorption

Table 7. The peak areas of ethanol and internal standard n-propanol in A sample

Sample A	Ethanol peak area, A_P	Propanol peak area, A_P	A_E/A_P	$K \cdot (A_E/A_P) \cdot m_P$
1	32074	73645	0,4355218	0,038486187
2	45893	108342	0,4235938	0,037432137
3	13777	32674	0,4216502	0,037260389
4	44506	106522	0,4178104	0,03692107
5	17220	41307	0,4168785	0,036838719
6	9432	25683	0,3672468	0,032452867

The properties of ethanol and internal standard n-propanol are listed in following table (8). The volume of the n-propanol was 0.02 ml as an internal standard in the mixture.

Table 8. Properties of ethanol and internal standard n-propanol

Reagent	Density, ρ ($\frac{g}{cm^3}$)	Volume, V (mL)	Mass, m (g)
Ethanol	0.7893 (20 °C)	20, $V_{\Delta ethanol} = 0.05$	2.0
N-propanol	0.8036 (20 °C)	$0.1, V_{\Delta propanol} = 0.02 (= 20\ \mu L)$,	-

The following equation (5) is an example for calculating the amount of ethanol adsorption in the mixture including internal standard propanol. The equation 6 was used to calculate the amount of mass of n-propanol. The leftover amount of ethanol adsorption in a certain period time was calculated to used equation 7.

5 Calibration equation

$$y = kx + b$$

$$\longrightarrow y = \frac{m_E}{m_P} = K \cdot \frac{A_E}{A_P} + b$$

$$\rightarrow m_E = m_P \cdot \left(K \cdot \frac{A_E}{A_P} + b\right)$$

whereas, y-axis intercept of mass ratio and x-axis intercept of area ratio, k coefficient, A_E area of ethanol, A_P area of propanol, b constant, m_E the mass of ethanol and m_p the mass of propanol.

6 Calculating the mass of internal standard propanol (m_P) by using the following equation below:

$$\rho = \frac{m}{V}$$

$$\rightarrow m_P = \rho_P \cdot V_P = 0.8036 \frac{g}{mL} \cdot 0.1\ mL = 0.08036\ g$$

Whereas, ρ density, m mass and V volume.

To continue calculating the mass of ethanol using equation (5), where b constant will not be considered:

$$\rightarrow m_E = m_P \cdot \left(K \cdot \frac{A_E}{A_P}\right)$$

$$m_E = 0.08036\ g \cdot \left(1.1046 \cdot \frac{32074}{73645}\right) = 0.038486\ g$$

7 The leftover amount of ethanol adsorption in a certain period time:

$$m_{\text{known ethanol}} = m_{\text{Leftover ethanol}} + m_{\Delta\text{ethanol}}$$

$$\rightarrow m_{\text{Leftover ethanol}} = m_{\Delta\text{ethanol}} - m_{\text{known ethanol}}$$

$$\rightarrow m_{\text{Leftover ethanol}} = (\rho_E \cdot V_E) - m_P \cdot \left(K \cdot \frac{A_E}{A_P}\right)$$

$$m_{\text{Leftover ethanol}} = m_{E,\text{left}} = (0.79 \cdot 0.05) - 0.038486\ g = 0.001013813\ \frac{adsorption}{g}$$

8 Calculation of the leftover of ethanol concentration (adsorption / g):

$$c_E = \frac{m_{E,\text{left}}}{2.0\ \text{g}} \cdot \rho_p \cdot V_{\Delta\text{propanol}} = \frac{0.001013813\ \frac{g}{g}}{2.0\ g} \cdot 0.8036\ \frac{g}{mL} \cdot 0.02\ mL$$

$$= 0.0005069065 \cdot 1000 \cdot 20\ \frac{mg}{g} = 10.13813 \approx 10\ \frac{mg}{g}$$

The adsorbed amounts of ethanol in the mixture are listed in the table below (9). For the rest of the samples the results are tabled and listed in the appendixes 12, 13 and 14.

Table 9. Adsorbed amount of ethanol in Nano-sized silicalite-1

Adsorption / g	mg/g-zeolite	Time (min)
0,001013813	10,13813131	10
0,002067863	20,67862657	30
0,002239611	22,39611434	60
0,00257893	25,78930099	120
0,002661281	26,61281139	240
0,007047133	70,47133279	1200 = 20h

The adsorption testing was shown in the Figure 21. As compared the sample A of Nano-sized zeolites and sample B of micro-sized zeolites synthesized from OH^- system. Sample A had smaller adsorbed amounts than sample B indicating the larger crystal. It is more beneficial for adsorption of ethanol. This is probably because of the large crystal with fewer defects and it is more hydrophobic having beneficial to the uptake of ethanol in its micro-pores. The same result was obtained for the sample C of large-sized zeolites and sample D of small-sized zeolites synthesized from F^--system. The larger size of zeolite has better adsorption performance than the rest of the samples.

Comparing the synthesized samples to each other, the samples (A & B) from hydroxide basic system and samples (C & D) from fluoride based on neutral system, the samples from F^--system had larger amounts of adsorbed ethanol than the samples from OH^- system. The adsorption rate of the samples from F^--system were higher than the synthesized samples from OH^--system. This indicates that the synthesized samples from fluoride neutral method have fewer defects, better adsorption performance and hydrophobic properties than the samples from hydroxide basic system.

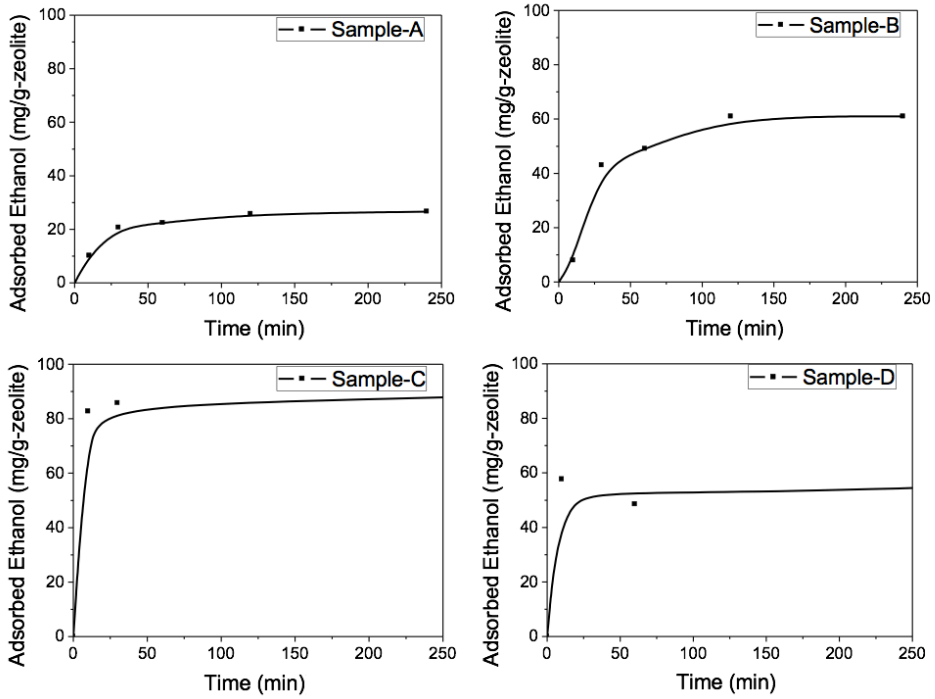

Figure 21. Adsorbed ethanol in the mixture using GC

8 CONCLUSION

In this experiment, the aim of the project was to adsorb ethanol from diluted aqueous solution, which has potential application in bio-ethanol separation. Four types of zeolites were synthesized based on their X-ray diffraction (XRD), scanning electronic microscopy (SEM) and nitrogen adsorption characterization, which was applied in ethanol adsorption testing.

Nano-sized silicalite-1 and micro-sized silicalite-1 were carried out with hydroxide (OH^-) system and large-sized silicalite-1 and small-sized silicalite-1 with hydrogen fluoride (F^-) method. After that, they were tested by powder X-ray diffraction equipment. The powder X-ray diffraction patterns demonstrated that every samples had the framework type MFI (MFI-framework, which belongs to pentasil zeolite family including ZSM-5) structure with crystallization and high purity. The samples carried out with F^--system were better crystallized and had higher intensity diffractions than the samples with OH^--system.

Scanning electronic microscope (SEM) images of Nano-sized silicalite-1 particles showed the uniform crystal sizes of 100–200 nm and their shapes were difficult to determine. SEM of micro-sized silicalite-1 particles had uniform crystal sizes about 1.0 μm and plate-like shapes. Large-sized silicalite-1 particles had also plate-like shapes and were notably bigger than micro-sized particles. Small-sized particles had no uniform sizes that may be because of an error or small amount of impurities in their particles. Scanning electronic microscope (SEM) images showed the cubic morphology and uniform crystal sizes between 1.0–5.0 μm and 100–200 nm differing with different images and samples.

Nitrogen adsorption-desorption isotherms demonstrated that the materials were type-I adsorption isotherms indicating microporous materials. The Langmuir adsorption isotherm known as type-1 adsorption isotherm is used to model monolayer formations in the graphs. As we can see from the results (Figure 17) type-1 isotherm describes a rapid rise approaching a maximum value asymptotically as the vapour pressure increases in the adsorption isotherms diagram. This indicates the amount of the adsorbed ethanol molecules at the maximum of surface area interacting with the adsorbent.

The ethanol concentration adsorption testing by gas chromatography showed that Nano-sized zeolites and micro-sized zeolites synthesized from OH^- system, had smaller adsorbed amounts than large-sized and small-sized zeolites. This indicated the larger crystallization, which is more beneficial for adsorption of ethanol. This was probably because of the large crystal with fewer defects and it is more hydrophobic. It is beneficial to the uptake of ethanol in its micro-pores. After all, the results indicated the samples, which carried out in F^--system had larger size of zeolite and better adsorption performance.

The experiment was carried out with two different methods (OH^-- and F^--system) and the sizes of each samples were compared to each other. Hydrophobic zeolites were chosen to adsorb selectively ethanol because it has more hydrophobicity than water. Finally, adsorption testing showed that the performance of hydrophobic zeolites was better than ordinary zeolites. The adsorption results were consistent and showed that hydrophobic zeolites have a good performance. Hydrophobic zeolites can be used in removal of organic pollution from water, separation of two types of substance with different polarity and adsorption alcohol from water the same as catalyst cracker (FCC) in the petrochemical and refining industries. They are also used in detergents to remove the stains and oil. The adsorption is based on the physical adsorption. It is happened on the surface of the materials by van der Waals forces.

The results were the guideline to search for suitable porous materials with hydrophobic property to adsorb ethanol from water. The experiment can be continued further to prepare more hydrophobic materials with high adsorption performance. The needs of hydrophobic zeolites will rise in the future, e.g., in the cleaning of air pollution and purifying water all over the world, especially in the developing countries.

REFERENCES

Alcohol (ethanol) chemical and physical properties. Chemical properties of ethanol. Image taken 12.9.2016.
http://www.nutrientsreview.com/alcohol/definition-physical-chemical-properties.html

Anderson M.W., Felix V. & Rocha J. 1996. Microporous titanosilicates and other novel zeolite-types solids. Manchester. Department of chemistry, U.K., 35–36.

Anger I. & Ulmanu M. 2012. Handbook of zeolites. Physical and chemical properties. Vassils J. Inglezakis and Antonis A. Zorpas editions. Panteltmon. Bentham Science Publishers.

Anuwattana R. & Khummongkol P. 2009. Handbook of zeolites. Synthesis of zeolites from industrial wastes.T.W. Wong's edition. Bankok. Nova Science Publishers, Inc.

Auerbach S. M., Carrado K. A. & Dutta P. K. 2003. Handbook of Zeolite Science and Technology. New York. Marcel Dekker, Inc.

Bioethanol for transportation. 2016. Read 13.9.2016.
http://www.esru.strath.ac.uk/EandE/Web_sites/02-03/biofuels/what_bioethanol.htm

Biomedical 2016. Tetraethyl orthosilicate. Captured image 18.10.2016.
http://www.mpbio.com/images/product-images/molecular-structure/02156788.png

Campelo J. & Clark J. & Luque R. 2011. Handbook of biofuels production. Vegetable–based feedstocks for biofuels production. New Delhi. Wood Publishing Limited.

Carbohydrates. Read 13.9.2016.
https://hackpad.com/ep/pad/static/K9fOB3rWkfP

Chen J., Huo Q., Pang W., Xu R., etc. 2007. Chemistry of Zeolites and Related Porous Materials. Synthesis and Structure. Singapore. John Wiley & Sons (Asia) Pte Ltd.

Dartt C.B. & Davis M.E. 1994. Applications of zeolites to fine chemicals synthesis. California. Elsevier Science B.V. All rights reserved, 151–156.

Dayah M. 2016. Periodic Table. Read 25.9.2016.
http://www.ptable.com/

Degnan F. T. 2000. Applications of zeolites in petroleum refining. New Jersey. J.C. Baltzer AG. Science Publishers, 349–350.

Emptage M., Zhao L. & Gray K.A. 2006. Bioethanol. Elsevier Ltd. All rights reserved, 141–142.

Facts about hydrogen fluoride. 2013. Centres of disease control and prevention. Emergency preparedness and response. Read 26.9.3016.
https://emergency.cdc.gov/agent/hydrofluoricacid/basics/facts.asp

Fletcher A. 2008. Porosity and sorption behaviour. Read 30.11.2016
http://personal.strath.ac.uk/ashleigh.fletcher/adsorption.htm

Gilson J.P. & Guisnet M.2002. Zeolites for cleaner technologies: catalytic science series. London. Imperial College Press, 3–5.

Illingworth J.A. n.d. Universty of Leeds Faculty of Biological Sciences.
http://www.bmb.leeds.ac.uk/illingworth/questions/

Inglezakis V.J. & Loizidou M.D. 2012. Handbook of Natural Zeolites. Bacau. SC European Focus Consulting SRL, 3–10, 24–30.

Leavens B. P. 2016. Zeolites. Chemistry explained. Read 29.8.2016.
http://www.chemistryexplained.com/Va-Z/Zeolites.html

Lower S. 2013. Hard water and hard softening. Vancouver. Read 26.10.2016.
http://www.chem1.com/CQ/hardwater.html

Naderi M. 2015. Surface Area: Brunauer-Emmett-Teller (BET). London. Surface measurement systems, Ltd., 585–589.

Penoncello S.G., Schroeder J.A. & Schroeder J.S. 2014. A fundamental equation of state for ethanol. Center for applied thermodynamic studies. University of Idaho. Moscow. AIP Publishing, 4–10.

Peskov M. 2016. Chemistry of Zeolite. Stockholm. Stockholm university. Read. 12.9.2016.
http://asdn.net/asdn/chemistry/zeolites.php

Pubchem.2016. Open chemistry database: ethanol. Read 25.9.2016.
https://pubchem.ncbi.nlm.nih.gov/compound/702

The commission on natural zeolites. 2005. Index of natural zeolites datasheets. Captured image 20.10.2016.
http://www.iza-online.org/natural/Datasheets/Chabazite/chabazite.htm

Thet K. & Woo N. 2013. Chemistry libretexts. Gas chromatography. Read 15.11.2016.
http://chem.libretexts.org/Core/Analytical_Chemistry/Instrumental_Analysis/Chromatography/Gas_Chromatography

Virta R. nd. Natural and synthetic zeolites. Read 20.9.2016.
http://minerals.usgs.gov/mineralofthemonth/zeolites.pdf

Woodford C. 2016. Zeolites. Read. 29.09.2016.
http://www.explainthatstuff.com/zeolites.html

Wong T.W. 2009. Hand book of Zeolites: Structure, Properties and applications. New York. Nova Science Publishers, Inc., 23–25.

Zeocem. About Zeolite. 18.9.2016.
http://www.zeocem.com/about-zeolite/

APPENDICES

Appendix 1. Properties of hydrogen fluoride (Pubchem 2016)

Cas-number	7664–39–3
Formula	HF
Molecular weight	20.01 g / mol
Density	1.15 g / ml (25 ℃)
Boiling point	19.5 ℃

Appendix 2. Properties of TEOS (Pubchem 2016)

Cas-number	78–10–4
Formula	$Si(C_2H_5O)_4$
Molecular weight	208.329 g / mol
Density	0.933 g / ml (20 ℃)
Boiling point	168.8 ℃

Appendix 3. Properties of TPAOH (Chemicalbook 2016)

Cas-number	4499–86–9
Formula	$C_{12}H_{29}NO$
Molecular weight	203.36 g / mol
Density	1.00 g / ml (20 ℃)
Boiling point	101 ℃

Appendix 4. Equipment information

Equipment	Company	Model	Brand
Autoclave	Qiang Qiang Shanghai Industrial Development Co., Ltd.	KH 100 ml	-
Centrifuge	Shanghai Anke Scientific Instrument company	model GL-20G-11	-
Electronic balance	Chang Zhou KeYi Electronic Instrument Co., Ltd.	JA5003	KeYi
Electronic box resistance furnace	Shaoxing Shang Yu Dao Yan Guang Instrument Co., Ltd	XMT-800	-
Filtration equipment	Zhang Zhou KeTai Laboratory Instrument Co. Ltd.	SHK-11	-
Heating furnace	Shanghai Shuli YiQi YiBao Co., Ltd.	FX–202–3	-
Gas Chromatography	Lu Chuang company	GC-9860	-
Lab dancer	IKA company	-	IKA
Magnetic stirrer	Shanghai Siye Instrument Co., Ltd.	85–2	SiYe
Oil bath	Zhang Zhou KeTai Laboratory Instrument Co. Ltd	DF-101S	KeTai
Ultrasonic wave	Shen Zhen Jey Men Cleaning Instrument Co., Ltd	-	-

Appendix 5. Item details

Equipment	Company	Model	Voltage (kV)	Amper (mA)	CuKα-radiation (Å)
PXRD	Bruker AXS GmbH	D8 advance	40	40	1 l/4.15418
N_2-adsorption	Micromeritics Instrument Corporation	TrisStar II 3020	-	-	-
SEM	FEI company	Quanta 200	20–30	-	-

Appendix 6. Chemical reagent information

Chemical reagent	Concentration	Company
TEOS	98 wt. %	Aladdin
TPAOH	25 wt. %	Guang Fu Chemical reagent
HF	40 wt. %	Macklin Chemical reagent

Appendix 7. N_2-adsorption-desorption isotherms of Nano-sized silicalite-1 (A)

TriStar II 3020 2.00	TriStar II 3020	Serial #: 948	Page 1
Sample:	a		
Operator:	2		
Submitter:	5		
File:	D:\wangjg\9-28\001-171.SMP		
Started:	2016-9-29 11:	Analysis Adso	N2
Completed:	2016-9-29 17:	Analysis Bath	-195.850 °C
Report Time:	2016-9-30 10:	Thermal Corre	No
Sample Mass:	0.0916 g	Warm Free Sp	19.5473 cm³ Measured
Cold Free Space:	58.0030 cm³	Equilibration I	10 s
Low Pressure Dose:	None	Sample Densi	1.000 g/cm³
Automatic Degas:	No		
Comments: microporous materials and zeolites			
Summary Report			
Surface Area			
Single point surface area at P/Po = 0.225152699:	437.3137 m²/g		
BET Surface Area:	428.4610 m²/g		
Langmuir Surface Area:	585.7651 m²/g		
t-Plot Micropore Area:	273.8362 m²/g		
t-Plot External Surface Area:	154.6248 m²/g		
BJH Adsorption cumulative surface area of pores between 1.7000 nm and 300.0000 nm diameter:	134.114 m²/g		
BJH Desorption cumulative surface area of pores between 1.7000 nm and 300.0000 nm diameter:	161.7646 m²/g		
Pore Volume			
Single point adsorption total pore volume of pores less than 418.7003 nm diameter at P/Po = 0.995415	0.472212 cm³/g		
t-Plot micropore volume:	0.130638 cm³/g		
BJH Adsorption cumulative volume of pores between 1.7000 nm and 300.0000 nm diameter:	0.329923 cm³/g		
BJH Desorption cumulative volume of pores between 1.7000 nm and 300.0000 nm diameter:	0.337198 cm³/g		
Pore Size			
Adsorption average pore width (4V/A by BET):	4.40845 nm		
BJH Adsorption average pore diameter (4V/A):	9.8401 nm		
BJH Desorption average pore diameter (4V/A):	8.3380 nm		
DFT Pore Size			
Volume in Pores	<	0.522 nm	: 0.08805 cm³/g
Total Volume in Pores	<=	44.883 nm	: 0.36184 cm³/g
Total Area in Pores	>=	0.522 nm	: 414.936 m²/g
Nanoparticle Size:			
Average Particle Size	14.0036 nm		
MP-Method			
Cumulative surface area of pores between 0.31741 nm and 0.52000 nm hydraulic radius:	438.8321 m²/g		
Cumulative pore volume of pores between 0.31741 nm and 0.52000 nm hydraulic radius:	0.150576 cm³/g		
Average pore hydraulic radius (V/A):	0.34313 nm		

TriStar II 3020 2.00	TriStar II 3020 Version 2.00	Serial #: 948	Page 1	
Sample:	a			
Operator:	2			
Submitter:	5			
File:	D:\wangjg\9-28\001-171.SMP			
Started:	2016-9-29 11:11:22	Analysis Adsorptive:	N2	
Completed:	2016-9-29 17:06:03	Analysis Bath Temp.:	-195.850 °C	
Report Time:	2016-9-30 10:34:29	Thermal Correction:	No	
Sample Mass:	0.0916 g	Warm Free Space:	19.5473 cm³ Measured	
Cold Free Space:	58.0030 cm³	Equilibration Interval:	10 s	
Low Pressure Dose:	None	Sample Density:	1.000 g/cm³	
Automatic Degas:	No			
Comments: microporous materials and zeolites				
Isotherm Tabular Report				
	Relative Pressure (P/Po)	Absolute Pressure (mmHg)	Quantity Adsorbed (cm³/g STP)	Elapsed Time	Saturation Pre
				00:38	762,681946
	4,3098E-05	0,032862373	1,436553785	00:46	762,502258
	6,46408E-05	0,049293563	2,004993523	00:50	762,575989
	0,000111225	0,084784925	63,2406685	00:59	762,282654
	0,044196031	33,68606949	114,9051557	01:04	762,196716
	0,05624856	42,87274551	115,8991756	01:07	762,20166
	0,08703212	66,33220673	118,0694389	01:10	762,157776
	0,121320949	92,46240234	120,3768819	01:13	762,130554
	0,156149483	118,9910431	122,901503	01:17	762,032898
	0,190578883	145,2019043	125,9102093	01:21	761,899231
	0,225152699	171,5318909	129,6487885	01:26	761,846924
	0,261616628	199,3157196	133,2464613	01:31	761,861816
	0,298195936	227,1644592	135,7803765	01:35	761,795959
	0,333920893	254,3335876	137,6222761	01:38	761,658203
	0,364208692	277,4026489	138,7468977	01:41	761,658508
	0,398622484	303,5904846	139,7238225	01:44	761,598999
	0,433650727	330,275238	140,4804221	01:46	761,615784
	0,468505497	356,8413696	141,1055241	01:48	761,658875
	0,503629643	383,5398865	141,6337668	01:50	761,551453
	0,538465423	410,050293	142,1247278	01:53	761,516479
	0,573487197	436,6755676	142,59	01:55	761,439087
	0,608381586	463,224762	143,0260257	01:57	761,404968
	0,643240087	489,7481384	143,4854346	01:59	761,376892
	0,67840885	516,5071411	143,981119	02:01	761,35083
	0,713103408	542,9094238	144,519888	02:03	761,333374
	0,748051908	569,578064	145,197626	02:06	761,415161
	0,783249694	596,2785645	146,0252889	02:08	761,287964
	0,817993708	622,6769409	147,0983212	02:10	761,224609
	0,852416172	648,9551392	148,6950194	02:12	761,312561
	0,887292891	675,4473267	151,247481	02:15	761,245056
	0,921119237	701,1677246	155,7641009	02:18	761,212769
	0,930365239	708,0219727	157,8981589	02:22	761,015076
	0,934041114	710,8509521	158,84397	02:24	761,048889
	0,941251231	716,2405396	161,2661901	02:27	760,945129
	0,944802683	718,9525146	162,5445683	02:29	760,9552
	0,946450771	720,239563	163,3915185	02:31	760,98999
	0,950627626	723,3373413	165,347879	02:34	760,905029
	0,956954779	728,076416	169,6686748	02:39	760,826355
	0,995415085	756,9312134	305,283151	03:24	760,417664
	0,974188341	740,798584	294,9392717	03:29	760,426453
	0,9689944	736,8806152	284,5484322	03:36	760,459106
	0,965890148	734,4750366	273,327424	03:42	760,412598
	0,96311875	732,328186	257,4311515	03:51	760,371643
	0,955732652	726,6863403	211,1672006	04:09	760,344788
	0,948399056	721,038269	181,9434357	04:22	760,26886
	0,926485314	704,2825928	160,4099564	04:32	760,165955
	0,885460618	673,1137695	151,6076561	04:36	760,184875
	0,842453981	640,4396973	148,2789105	04:39	760,207336
	0,804577357	611,6749268	146,6550025	04:41	760,243774
	0,768602619	584,3041992	145,644949	04:43	760,216248
	0,733037487	557,2858887	144,8970338	04:46	760,242004
	0,716118857	544,4343872	144,583098	04:48	760,257019
	0,681600929	518,1781616	144,0857516	04:50	760,236877
	0,646700711	491,6334534	143,6485372	04:52	760,217896
	0,611524712	464,8910217	143,2584557	04:54	760,216248
	0,57645193	438,2156677	142,9029372	04:56	760,194641
	0,541304174	411,5287781	142,5476518	04:58	760,254211
	0,50623696	384,8533936	142,2081805	05:00	760,223816
	0,471188853	358,1975708	141,8592342	05:02	760,199585
	0,436136051	331,5404358	141,4647354	05:04	760,176636
	0,401005744	304,8432007	141,0174629	05:07	760,196594
	0,366082986	278,2841797	140,4134637	05:09	760,166931
	0,330808501	251,4719238	139,6839019	05:11	760,173706
	0,296005976	225,0136108	138,7016619	05:14	760,165771
	0,261193287	198,5424805	137,1949598	05:18	760,13623
	0,226511457	172,1791229	134,7093637	05:22	760,134277
	0,191890385	145,8672028	130,6342381	05:29	760,158997
	0,157987193	120,0704117	125,3921719	05:37	760,000916
	0,117540645	89,33274841	120,6206608	05:43	760,015808
	0,085487427	64,97302246	118,0039848	05:47	760,030151
	0,044660442	33,94371033	114,9323674	05:53	760,039734

Appendix 8. N_2-adsorption-desorption isotherms of micro-sized silicalite-1 (B)

TriStar II 3020 2.00	TriStar II 3020 V	Serial #: 948	Page 1
Sample:	b		
Operator:	3		
Submitter:	6		
File:	D:\wangjg\9-28\001-172.SMP		
Started:	2016-9-29 11:11	Analysis Adsorpti	N2
Completed:	2016-9-29 17:06	Analysis Bath Tei	-195.850 °C
Report Time:	2016-9-30 10:35	Thermal Correcti	No
Sample Mass:	0.1242 g	Warm Free Spac	20.4893 cm³ Measured
Cold Free Space:	60.8279 cm³	Equilibration Inter	10 s
Low Pressure Dose:	None	Sample Density:	1.000 g/cm³
Automatic Degas:	No		
Comments: microporous materials and zeolites			
Summary Report			
Surface Area			
Single point surface area at P/Po = 0.222965261:	401.2951 m²/g		
BET Surface Area:	393.8124 m²/g		
Langmuir Surface Area:	539.8902 m²/g		
t-Plot Micropore Area:	288.7778 m²/g		
t-Plot External Surface Area:	105.0346 m²/g		
BJH Adsorption cumulative surface area of pores between 1.7000 nm and 300.0000 nm diameter:	130.928 m²/g		
BJH Desorption cumulative surface area of pores between 1.7000 nm and 300.0000 nm diameter:	141.5564 m²/g		
Pore Volume			
Single point adsorption total pore volume of pores less than 242.3222 nm diameter at P/Po = 0.992038829:	0.194550 cm³/g		
t-Plot micropore volume:	0.135625 cm³/g		
BJH Adsorption cumulative volume of pores between 1.7000 nm and 300.0000 nm diameter:	0.069821 cm³/g		
BJH Desorption cumulative volume of pores between 1.7000 nm and 300.0000 nm diameter:	0.066406 cm³/g		
Pore Size			
Adsorption average pore width (4V/A by BET):	1.97607 nm		
BJH Adsorption average pore diameter (4V/A):	2.1331 nm		
BJH Desorption average pore diameter (4V/A):	1.8764 nm		
DFT Pore Size			
Volume in Pores	<	0.522 nm	0.05069 cm³/g
Total Volume in Pores	<=	44.883 nm	0.20020 cm³/g
Total Area in Pores	>=	0.522 nm	583.532 m²/g
Nanoparticle Size:			
Average Particle Size	15.2357 nm		
MP-Method			
Cumulative surface area of pores between 0.19706 nm and 0.52000 nm hydraulic radius:	627.2743 m²/g		
Cumulative pore volume of pores between 0.19706 nm and 0.52000 nm hydraulic radius:	0.166710 cm³/g		
Average pore hydraulic radius (V/A):	0.26577 nm		

TriStar II 3020 2.00	TriStar II 3020 Versior	Serial #: 948	Page 1
Sample:	b		
Operator:	3		
Submitter:	6		
File:	D:\wangjg\9-28\001-172.SMP		
Started:	2016-9-29 11:11:22	Analysis Adsorptive:	N2
Completed:	2016-9-29 17:06:03	Analysis Bath Temp.:	-195.850 °C
Report Time:	2016-9-30 10:35:34	Thermal Correction:	No
Sample Mass:	0.1242 g	Warm Free Space:	20.4893 cm³ Measured
Cold Free Space:	60.8279 cm³	Equilibration Interval:	10 s
Low Pressure Dose:	None	Sample Density:	1.000 g/cm³
Automatic Degas:	No		
Comments: microporous materials and zeolites			
Isotherm Tabular Report			

Relative Pressure (P/Po)	Absolute Pressure (m	Quantity Adsorbed (cm³/g STP)	Elapsed Time	Saturation Pressure (mmHg)
			00:38	762,681946
4,49432E-05	0,0342745	0,290945748	00:42	762,616943
6,61819E-05	0,050466534	0,938113008	00:45	762,54187
0,000112422	0,085727356	13,08479548	00:50	762,546326
0,00026989	0,205729201	86,76288624	01:01	762,271301
0,046238744	35,24487305	103,5315692	01:06	762,236816
0,056648645	43,17568207	104,0154249	01:09	762,166199
0,087958336	67,03961182	105,4277849	01:13	762,174622
0,120457039	91,79681396	107,1260864	01:17	762,070984
0,154977298	118,0683441	109,5732018	01:23	761,842834
0,187906859	143,1416626	113,8843444	01:34	761,769226
0,222965261	169,8055878	118,635556	01:45	761,578674
0,261669165	199,2698212	121,9612041	01:53	761,533447
0,301690285	229,7241516	123,7020946	01:58	761,456909
0,335943006	255,7653809	124,4796423	02:02	761,335632
0,382606177	291,2806702	125,0562789	02:05	761,306763
0,418301444	318,4949341	125,3147069	02:07	761,400513
0,453557668	345,302887	125,4492617	02:10	761,320801
0,488591886	371,9715576	125,5065093	02:12	761,313416
0,523663	398,618866	125,5162064	02:14	761,212585
0,55869131	425,2292175	125,4710625	02:16	761,116577
0,593596578	451,8096008	125,3991296	02:18	761,13916
0,628462459	478,3627319	125,3093988	02:20	761,163574
0,663604659	505,0301208	125,204219	02:22	761,040649
0,698384583	531,5529785	125,0864343	02:24	761,117859
0,733567388	558,1984863	124,9518533	02:27	760,93689
0,768174434	584,5803223	124,8280734	02:29	760,999451
0,803086797	611,1669922	124,6983438	02:31	761,022339
0,838388836	637,9786987	124,5802733	02:33	760,958008
0,873206808	664,5352173	124,4902901	02:35	761,028442
0,908001809	690,8989868	124,4447579	02:37	760,900452
0,942325991	717,1036377	124,5293033	02:39	760,993164
0,943049709	717,4597168	124,5420355	02:42	760,786743
0,944786295	718,8237915	124,5556795	02:44	760,832153
0,965053157	734,1643066	124,7634404	02:46	760,750122
0,992038829	754,6323242	125,7758273	02:48	760,688293
0,961748921	731,5317993	124,7948024	02:50	760,626587
0,942012518	716,5741577	124,564866	02:53	760,684326
0,908074969	690,6797485	124,4807806	02:55	760,597717
0,872530119	663,6256714	124,5107144	02:57	760,576233
0,837354719	636,8345337	124,5946661	02:59	760,531372
0,802140336	610,0629272	124,7013949	03:01	760,543884
0,767009217	583,357605	124,8260214	03:03	760,561401
0,731849067	556,675293	124,9603971	03:05	760,642212
0,696950964	530,0438843	125,0884088	03:07	760,518188
0,661689193	503,2702026	125,2222764	03:10	760,583984
0,626668315	476,6411133	125,3386051	03:12	760,59552
0,59161407	449,9842834	125,4449336	03:14	760,604431
0,556617502	423,2989807	125,5538817	03:16	760,484497
0,521528179	396,5980835	125,6224311	03:18	760,453796
0,486437328	369,9261169	125,6713244	03:20	760,48053
0,4514795	343,3078613	125,6807272	03:22	760,406311
0,416422813	316,6622009	125,6377277	03:24	760,434326
0,400523154	304,5551758	125,5852426	03:27	760,393433
0,365974642	278,2813416	125,4969928	03:29	760,384216
0,330987887	251,7083282	125,3440774	03:31	760,475952
0,295868554	224,9916382	125,1057694	03:33	760,44458
0,260819328	198,3469543	124,7433972	03:36	760,47644
0,225881023	171,7696686	124,1646998	03:40	760,443115
0,191533311	145,6482239	122,9374817	03:46	760,432861
0,159694417	121,4311905	119,2333511	04:00	760,397217
0,125671204	95,54465485	110,1457441	04:16	760,274841
0,086464204	65,73635864	105,6182123	04:23	760,272522
0,045982485	34,95489502	103,7	04:29	760,178467

Appendix 9. N_2-adsorption-desorption isotherms of large-sized silicalite-1 (C)

TriStar II 3020 2.00	TriStar II 3020	Serial #: 948	Page 1
Sample:	c		
Operator:	1		
Submitter:	1		
File:	D:\wangjg\9-28\001-173.SMP		
Started:	2016-9-29 18:4	Analysis Adso	N2
Completed:	2016-9-29 23:1	Analysis Bath	-195.850 °C
Report Time:	2016-9-30 10:3	Thermal Corre	No
Sample Mass:	0.0694 g	Warm Free Sp	20.3708 cm³ Measured
Cold Free Space:	59.1670 cm³	Equilibration I	10 s
Low Pressure Dose:	None	Sample Densi	1.000 g/cm³
Automatic Degas:	No		
Comments: microporous materials and zeolites			
Summary Report			
Surface Area			
Single point surface area at P/Po = 0.224562508:	375.6722 m²/g		
BET Surface Area:	374.7116 m²/g		
Langmuir Surface Area:	514.1363 m²/g		
t-Plot Micropore Area:	260.5561 m²/g		
t-Plot External Surface Area:	114.1555 m²/g		
BJH Adsorption cumulative surface area of pores between 1.7000 nm and 300.0000 nm diameter:	163.573 m²/g		
BJH Desorption cumulative surface area of pores between 1.7000 nm and 300.0000 nm diameter:	39.6484 m²/g		
Pore Volume			
Single point adsorption total pore volume of pores less than 198.4716 nm diameter at P/Po = 0.990255692:	0.202549 cm³/g		
t-Plot micropore volume:	0.119868 cm³/g		
BJH Adsorption cumulative volume of pores between 1.7000 nm and 300.0000 nm diameter:	0.102144 cm³/g		
BJH Desorption cumulative volume of pores between 1.7000 nm and 300.0000 nm diameter:	0.037337 cm³/g		
Pore Size			
Adsorption average pore width (4V/A by BET):	2.16218 nm		
BJH Adsorption average pore diameter (4V/A):	2.4978 nm		
BJH Desorption average pore diameter (4V/A):	3.7668 nm		
DFT Pore Size			
Volume in Pores	<	0.522 nm	0.00000 cm³/g
Total Volume in Pores	<=	44.883 nm	0.20389 cm³/g
Total Area in Pores	>=	0.522 nm	796.033 m²/g
Nanoparticle Size:			
Average Particle Size	16.0123 nm		
MP-Method			
Cumulative surface area of pores between 0.22063 nm and 0.54000 nm hydraulic radius:	593.7593 m²/g		
Cumulative pore volume of pores between 0.22063 nm and 0.54000 nm hydraulic radius:	0.181453 cm³/g		
Average pore hydraulic radius (V/A):	0.30560 nm		

TriStar II 3020 2.00	TriStar II 3020 Version 2.	Serial #: 948	Page 1	
Sample:	c			
Operator:	1			
Submitter:	1			
File:	D:\wangjg\9-28\001-173.SMP			
Started:	2016-9-29 18:46:03	Analysis Adsorptive:	N2	
Completed:	2016-9-29 23:16:03	Analysis Bath Temp.:	-195.850 °C	
Report Time:	2016-9-30 10:36:15	Thermal Correction:	No	
Sample Mass:	0.0694 g	Warm Free Space:	20.3708 cm³ Measured	
Cold Free Space:	59.1670 cm³	Equilibration Interval:	10 s	
Low Pressure Dose:	None	Sample Density:	1.000 g/cm³	
Automatic Degas:	No			
Comments: microporous materials and zeolites				
Isotherm Tabular Report				

Relative Pressure (P/Po)	Absolute Pressure (mmH	Quantity Adsorbed (cm³/g STP)	Elapsed Time (h:m	Saturation Pressure (mmHg)
			00:47	761,066956
3,76134E-05	0,02863331	1,052768654	00:50	761,251465
6,9607E-05	0,053000338	4,226357406	00:54	761,421692
0,000122608	0,093365915	33,36858546	00:58	761,497437
0,001445155	1,100618482	85,90195912	01:04	761,592102
0,002597024	1,97807765	87,02214224	01:08	761,670837
0,005295121	4,033276081	88,57873076	01:13	761,696716
0,009558877	7,281393051	89,83699155	01:17	761,741455
0,014293459	10,88787746	90,63991921	01:20	761,738464
0,0316317	24,09513474	92,31903927	01:23	761,740112
0,049222097	37,49601364	93,52795001	01:26	761,771973
0,084301393	64,21852112	95,50221252	01:28	761,772949
0,120914969	92,10851288	97,167914	01:31	761,762695
0,153006144	116,5621796	101,1313667	01:37	761,813721
0,18665158	142,1931763	107,3838235	01:43	761,81073
0,224562508	171,0645752	111,2893887	01:47	761,768188
0,261860388	199,4684906	113,8721679	01:50	761,736023
0,298208088	227,156662	115,3756536	01:53	761,73877
0,331738824	252,6962585	116,5223793	01:56	761,732544
0,364182081	277,4245911	117,4444415	01:58	761,774414
0,399079412	304,0092773	118,296416	02:00	761,793579
0,434011099	330,6315308	119,0550532	02:02	761,804321
0,46898516	357,274292	119,72777	02:04	761,802979
0,503955735	383,8991699	120,3124992	02:06	761,771606
0,538548371	410,2580566	120,8526841	02:08	761,784973
0,573556627	436,921814	121,353219	02:10	761,776245
0,608395019	463,4562683	121,84	02:12	761,768677
0,643403062	490,1077271	122,3088981	02:15	761,74292
0,678542472	516,8792725	122,7760247	02:17	761,749329
0,713480064	543,5125122	123,2338589	02:19	761,776733
0,748066223	569,8919067	123,6673329	02:21	761,820129
0,783159019	596,6643066	124,1220808	02:23	761,868652
0,818457979	623,5766602	124,6199043	02:25	761,89209
0,853664117	650,368103	125,1370996	02:27	761,854797
0,888270571	676,7437134	125,7513178	02:30	761,866638
0,922963056	703,1610718	126,4702551	02:32	761,851807
0,929100488	707,8413086	126,6712263	02:34	761,856567
0,933637407	711,2874756	126,8222692	02:36	761,84552
0,941900335	717,6127319	127,061134	02:38	761,877563
0,94457007	719,6365967	127,1632998	02:40	761,866821
0,946832402	721,3508301	127,2596741	02:42	761,856934
0,95133522	724,7543335	127,4596397	02:44	761,828552
0,959370253	730,9155273	127,8130472	02:46	761,870117
0,990255692	754,4205933	130,9468967	02:49	761,844238
0,9623816	733,1802368	128,2164328	02:51	761,839417
0,942653898	718,1652222	127,307988	02:53	761,854614
0,924480408	704,3565674	126,7905122	02:56	761,894531
0,89257103	680,0505981	126,154635	02:58	761,900818
0,857482169	653,3528442	125,6197484	03:00	761,943359
0,822086545	626,4020996	125,1442065	03:02	761,966125
0,787176941	599,809082	124,756007	03:04	761,974915
0,752217814	573,1374512	124,3874776	03:06	761,930176
0,717032818	546,3161621	124,0506053	03:08	761,912354
0,681975384	519,5990601	123,7136012	03:10	761,902954
0,646834108	492,8174744	123,3897043	03:12	761,891602
0,611473852	465,896759	123,0453781	03:14	761,924255
0,576628127	439,355896	122,7170896	03:16	761,939758
0,541569181	412,6670227	122,3776767	03:19	761,983948
0,50622198	385,7362976	122,0084032	03:21	761,990417
0,471469369	359,2664795	121,5319692	03:23	762,014465
0,436325018	332,5065613	120,8987591	03:25	762,061646
0,400917269	305,5296936	120,4134898	03:27	762,07666
0,36623399	279,1220703	119,9231168	03:29	762,141357
0,331002187	252,2804565	119,3908901	03:31	762,17157
0,295879579	225,5185699	118,8159772	03:33	762,197144
0,26066063	198,6759491	118,1553906	03:36	762,201599
0,225578963	171,9434204	117,3764128	03:38	762,231628
0,190532002	145,2151794	116,4338875	03:41	762,156372
0,155687778	118,65	115,063983	03:43	762,102417
0,124008069	94,50468445	104,9434588	03:57	762,084961
0,087593666	66,77057648	93,48297476	04:03	762,276306
0,043649748	33,27354431	92,13570314	04:08	762,284912

Appendix 10. N_2-adsorption-desorption isotherms of small-sized silicalite-1 (D)

TriStar II 3020 2.00	TriStar II 3020 V	Serial #: 948	Page 1		TriStar II 3020 2.00	TriStar II 3020 Ver	Serial #: 948	Page 1	
Sample:	d				Sample:	d			
Operator:	2				Operator:	2			
Submitter:	2				Submitter:	2			
File:	D:\wangjg\9-28\001-174.SMP				File:	D:\wangjg\9-28\001-174.SMP			
Started:	2016-9-29 18:46	Analysis Adso	N2		Started:	2016-9-29 18:46:0	Analysis Adsorptive:	N2	
Completed:	2016-9-29 23:16	Analysis Bath	-195.850 °C		Completed:	2016-9-29 23:16:0	Analysis Bath Temp.:	-195.850 °C	
Report Time:	2016-9-30 10:37	Thermal Corre	No		Report Time:	2016-9-30 10:37:2	Thermal Correction:	No	
Sample Mass:	0.0747 g	Warm Free Sp	20.6313 cm³ Measured		Sample Mass:	0.0747 g	Warm Free Space:	20.6313 cm³ Measured	
Cold Free Space:	60.2341 cm³	Equilibration I	10 s		Cold Free Space:	60.2341 cm³	Equilibration Interval:	10 s	
Low Pressure Dose:	None	Sample Densi	1.000 g/cm³		Low Pressure Dose:	None	Sample Density:	1.000 g/cm³	
Automatic Degas:	No				Automatic Degas:	No			
Comments: microporous materials and zeolites					Comments: microporous materials and zeolites				
Summary Report					Isotherm Tabular Report				
					Relative Pressure (P/Po)	Absolute Pressure	Quantity Adsorbed (cm³/g STP)	Elapsed Time (h:	Saturation Pressure (m
								00:47	761,0669556
Surface Area					3,56152E-05	0,02711146	0,188993091	00:50	761,2318115
					7,94099E-05	0,06046677	5,871816703	00:54	761,4509277
Single point surface area at P/Po = 0.223049078:	375.2998 m²/g				0,000133781	0,101873361	51,79430648	01:02	761,4923096
					0,027264852	20,76556969	90,73348443	01:06	761,6241455
BET Surface Area:	375.3604 m²/g				0,036788541	28,02010345	91,27710431	01:08	761,6530151
					0,056477252	43,01651764	92,21169046	01:11	761,6609497
Langmuir Surface Area:	525.1867 m²/g				0,085454143	65,09132385	93,39493124	01:13	761,7105713
					0,120657556	91,90932465	94,6	01:16	761,7369995
t-Plot Micropore Area:	281.2318 m²/g				0,155059498	118,1114807	96,44685338	01:20	761,7171631
					0,204409349	155,710144	109,1456887	01:33	761,7564697
t-Plot External Surface Area:	94.1286 m²/g				0,223049078	169,9204865	110,9625086	01:36	761,8076172
					0,261439653	199,1698151	113,2990496	01:40	761,819458
BJH Adsorption cumulative surface area of pores					0,296272176	225,7042084	114,6748994	01:43	761,8137207
between 1.7000 nm and 300.0000 nm diameter:	166.458 m²/g				0,331484864	252,530426	115,7439366	01:45	761,8158569
					0,364099468	277,3635254	116,5466566	01:48	761,779541
BJH Desorption cumulative surface area of pores					0,398987582	303,9289856	117,2661584	01:50	761,7504883
between 1.7000 nm and 300.0000 nm diameter:	45.3632 m²/g				0,434007893	330,5995789	117,8838695	01:52	761,7363281
					0,468886783	357,1681824	118,4173457	01:54	761,7365112
					0,503832254	383,7903137	118,8454461	01:56	761,7422485
					0,538653146	410,3296204	119,257684	01:58	761,7696533
Pore Volume					0,573688871	437,0253906	119,6060387	02:00	761,781189
					0,608513911	463,5530396	119,9676096	02:03	761,7788696
Single point adsorption total pore volume of pores					0,643546928	490,2496033	120,2825682	02:05	761,7930908
less than 194.2389 nm diameter at P/Po = 0.9900	0.197945 cm³/g				0,678401576	516,8017578	120,5838105	02:07	761,7932739
					0,713438368	543,4966431	120,8855749	02:09	761,7990112
t-Plot micropore volume:	0.129179 cm³/g				0,748287412	570,0284424	121,1995373	02:11	761,7774048
					0,783047715	596,4849243	121,5321745	02:13	761,7478638
BJH Adsorption cumulative volume of pores					0,81807488	623,163147	121,8848168	02:16	761,7434082
between 1.7000 nm and 300.0000 nm diameter:	0.100198 cm³/g				0,852996334	649,7589722	122,2847676	02:18	761,7371216
					0,887849423	676,3677979	122,7708439	02:20	761,8046265
BJH Desorption cumulative volume of pores					0,922701309	702,9578857	123,4607467	02:22	761,8477173
between 1.7000 nm and 300.0000 nm diameter:	0.037240 cm³/g				0,92901075	707,7991943	123,6560972	02:24	761,8848267
					0,933502925	711,2127686	123,7987069	02:26	761,8752441
					0,941953195	717,6478882	124,0559164	02:28	761,8721313
					0,944747501	719,7527466	124,1685673	02:30	761,8466797
Pore Size					0,947160112	721,598938	124,2697299	02:32	761,8552856
					0,95117492	724,6585693	124,4189288	02:34	761,8562622
Adsorption average pore width (4V/A by BET):	2.10938 nm				0,959219067	730,7957764	124,8172975	02:36	761,8653564
					0,990039063	754,262146	127,9704097	02:39	761,8498535
BJH Adsorption average pore diameter (4V/A):	2.4078 nm				0,961956176	732,8759766	125,9045804	02:42	761,86
					0,942878684	718,3383179	124,7277633	02:44	761,8565674
BJH Desorption average pore diameter (4V/A):	3.2838 nm				0,92472453	704,4940796	124,0604851	02:46	761,8421021
					0,892293034	679,8068237	123,3711156	02:48	761,8649902
					0,857346643	653,1784668	122,881235	02:50	761,8604126
					0,822085626	626,3338623	122,5027114	02:52	761,8839722
DFT Pore Size					0,786926368	599,5299683	122,2171685	02:54	761,862854
					0,751784042	572,7805176	121,9760269	02:56	761,8950195
Volume in Pores	<	0.522 nm	0.00000 cm³/g		0,716706622	546,0696411	121,7296445	02:58	761,9151611
Total Volume in Pores	<=	44.883 nm	0.19500 cm³/g		0,681541313	519,2996216	121,4854047	03:00	761,9488525
Total Area in Pores	>=	0.522 nm	714.248 m²/g		0,646472207	492,5999451	121,2525003	03:02	761,9816284
					0,611450361	465,8926697	121,0372272	03:05	761,9468384
					0,576362092	439,1578369	120,8117822	03:07	761,9478149
Nanoparticle Size:					0,54127316	412,3991394	120,584381	03:09	761,9057617
					0,506165216	385,6613159	120,3446253	03:11	761,9277344
Average Particle Size	15.9846 nm				0,471469304	359,2141724	119,7534849	03:13	761,9036255
					0,435601207	331,8958435	119,3218232	03:15	761,9259033
					0,401017667	305,5591125	118,9579299	03:17	761,9592285
					0,36590612	278,802887	118,5738246	03:20	761,9519653
MP-Method					0,330731548	252,0276337	118,156946	03:22	762,0308228
					0,295716426	225,3405914	117,6696756	03:24	762,0158081
Cumulative surface area of pores between					0,260605643	198,5945587	117,0918	03:26	762,0501099
0.29585 nm and 0.52000 nm hydraulic radius:	402.9579 m²/g				0,225583337	171,9162292	116,3571377	03:28	762,0963135
					0,190594078	145,2628632	115,3365624	03:31	762,1583252
Cumulative pore volume of pores between					0,156493762	119,2802353	113,1017494	03:35	762,2044067
0.29585 nm and 0.52000 nm hydraulic radius:	0.143818 cm³/g				0,120593109	91,90209198	95,53286135	03:51	762,0841064
					0,085746078	65,34436798	91,50606474	03:54	762,0682983
Average pore hydraulic radius (V/A):	0.35691 nm				0,042954063	32,73995972	90,70524357	04:01	762,2086792

Appendix 11. The peak areas of ethanol and propanol in the sample B

Sample B	Ethanol peak area, A_E	Propanol peak area, A_P	A_E/A_P	$K \cdot (A_E/A_P) \cdot m_P$	Adsorption / g	mg/g-zeolite	Time (min)
1	15695	35838	0,437943	0,038700144	0,000799856	7,998560188	10
2	40711	102131	0,3986155	0,035224855	0,004275145	42,75145176	30
3	20280	51783	0,3916343	0,034607942	0,004892058	48,92058398	60
4	3461	9161	0,3777972	0,033385182	0,006114818	61,1481847	120
5	55799	147842	0,3774232	0,033352133	0,006147867	61,47867101	240
6	4069	19880	0,2046781	0,018086992	0,021413008	214,1300845	1500 = 25h

Appendix 12. The peak areas of ethanol and propanol in the sample C

Sample C	Ethanol peak area, A_E	Propanol peak area, A_P	A_E/A_P	$K \cdot (A_E/A_P) \cdot m_P$	Adsorption / g	mg/g-zeolite	Time (min)
1	13178	37290	0,3533923	0,031228573	0,008271427	82,71426549	10
2	8584	24528	0,3499674	0,030925918	0,008574082	85,74082192	30
3	81475	218512	0,3728628	0,032949141	0,006550859	65,50858534	240
4	4290	12776	0,3357858	0,029672724	0,009827276	98,27276143	1140 = 19h

Appendix 13. The peak areas of ethanol and propanol in the sample D

Sample D	Ethanol peak area, A_E	Propanol peak area, A_P	A_E/A_P	$K \cdot (A_E/A_P) \cdot m_P$	Adsorption / g	mg/g-zeolite	Time (min)
1	5922	15512	0,381769	0,033736159	0,005763841	57,63841155	10
2	41693	106334	0,3920947	0,034648626	0,004851374	48,51373747	60
3	19498	53445	0,3648237	0,032238736	0,007261264	72,61263654	1080 = 18h